CHALMERS
UNIVERSITY OF TECHNOLOGY

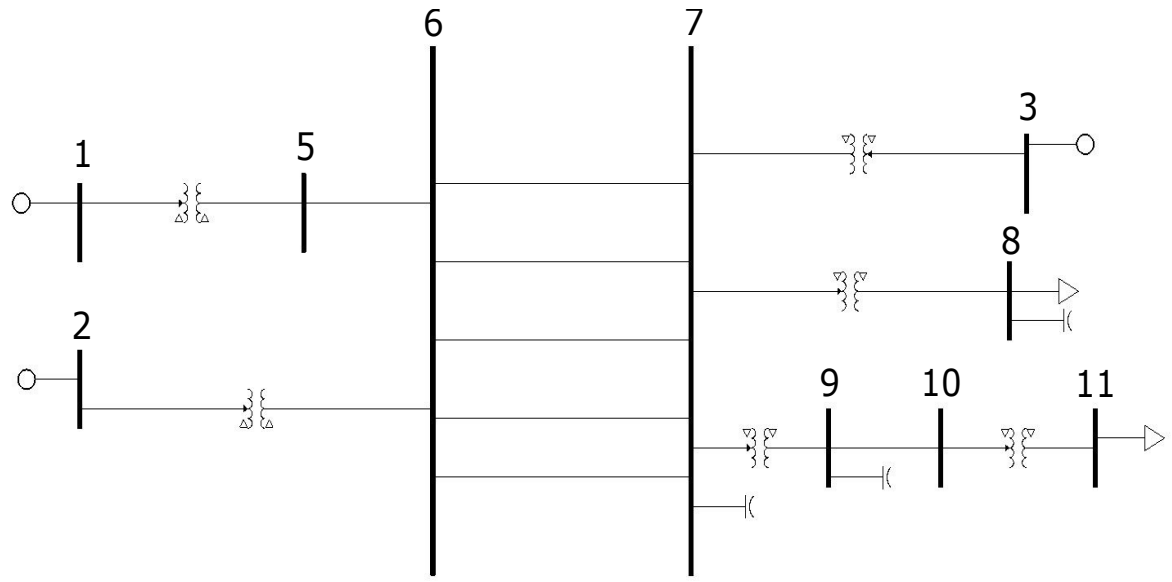

Load Model Identification and Parameter Estimation

Master's Thesis in Electric Power Engineering

MIRZA HAMIDOVIC AND MOHAMMAD FATEH KHOUDEIR

Department of Energy & Environment
CHALMERS UNIVERSITY OF TECHNOLOGY
Gothenburg, Sweden 2019

Master's Thesis 2019

Load Model Identification and Parameter Estimation

MIRZA HAMIDOVIC AND MOHAMMAD FATEH KHOUDEIR

CHALMERS
UNIVERSITY OF TECHNOLOGY

Department of Energy & Environment
Division of Electrical Power Engineering
Chalmers University of Technology
Gothenburg, Sweden 2019

Load Model Identification and Parameter Estimation
MIRZA HAMIDOVIC AND MOHAMMAD FATEH KHOUDEIR

Supervisor: Tarik Abdulahovic, ABB Power Consulting
Examiner: Anh Tuan Le, Department of Electric Power Engineering

Master's Thesis EENX30
Department of Energy & Environment
Division of Electrical Power Engineering
Chalmers University of Technology
SE-412 96 Gothenburg
Telephone +46 31 772 1000

Typeset in LaTeX
Printed by Chalmers University of Technology
Gothenburg, Sweden 2019

Load Model Identification and Parameter Estimation
MIRZA HAMIDOVIC AND MOHAMMAD FATEH KHOUDEIR
Department of Energy & Environment
Chalmers University of Technology

Abstract

The power system response during different grid events strongly depends on the load composition. For instance these events could be, faults which can cause disturbances in both voltage and frequency. Therefore, the need for having a reliable load model that helps to study and simulate the behaviour of the load is desired. The ZIP load model is a type of load model used by the Nordic TSOs. The main goal of this thesis is to improve existing ZIP load model by finding parameters that represent the load with a good accuracy, in other words, to increase the reliability of the test model to be used to simulate the real power system. Two main methods can be used for accurate estimation of the load model parameters, 'Component-based approach' and 'Measurement-based approach'. In this thesis, the later approach has been selected, the reason behind which is that large sets of measured data were provided by local DSO's. For the curve-fitting purposes, two algorithms have been applied: Genetic Algorithm (GA) and Particle Swarm optimization (PSO) algorithms. Since, the GA algorithm yields more reasonable results, the coefficients corresponding to this method were adopted as the reference against which results of other coefficients were compared. Finally, a test model was built and different combinations of the ZIP model were tested and compared with the reference after introducing voltage events.

Keywords: Load modelling, measurement-based approach, ZIP load model, curve-fitting, genetic algorithm, particle swarm optimization

Acknowledgements

This master thesis started in January 2019, and was completed in June the same year. Most of the research was conducted at the ABB facility in Mölndal, Sweden and the meetings where held at the Department of Electrical Engineering at Chalmers University of Technology.

First of all, we would like to thank ABB Consulting represented by Amer Omanovic for giving us this opportunity to do our thesis work in the esteemed company.

Special thanks to our supervisor Tarik Abdulahovic for his support and guidance throughout this work. We would also like to thank all the friendly colleagues with whom we had a nice time in ABB.

We would also like to express our gratitude to our examiner in Chalmers Anh Tuan Le for his valuable inputs to our work and constructive feedback.

MIRZA HAMIDOVIC AND MOHAMMAD FATEH KHOUDEIR, Gothenburg, June 2019

Contents

List of Figures

List of Tables

Acronyms

TSO Transmission system operator

DSO Distribution system operator

IEEE Institute of Electrical and Electronics Engineers

CIGRE International Council on Large Electric Systems

SQL Structured Query Language

RMS Root Mean Square

GA Genetic Algorithm

PSO Particle Swarm Optimization

Nomenclature

S Apparent power

P Active power

Q Reactive power

θ Displacement angle

DPF Displacement power factor

PF Power factor

THD Total harmonic distortion

Z_p Fraction of constant impedance load

I_p Fraction of constant current load

P_p Fraction of constant power load

Z_q Fraction of constant impedance load

I_q Fraction of constant current load

P_q Fraction of constant power load

U_0 Voltage initial value

P_0 Active power initial value

Q_0 Reactive power initial value

n_p Exponential load model parameter for active power

n_q Exponential load model parameter for reactive power

k_{pf} Load frequency sensitivity parameter

f Frequency

f_0 Nominal frequency

1
Introduction

OVER the past few decades, power systems simulation software have gained prominence as fundamental tools for reliable power systems operations. This interest towards accurate simulation software has especially grown after a number of critical accidents. One such example is the voltage collapse that took place in Sweden in 1983 [1]. This event and other similar events highlighted the necessity for developing accurate models for power system components. Moreover, finding effective solutions that ensure the secure power transfer of the power system increased the necessity for the constant improvement of power systems simulation software and models. In this regard, important research was carried on load modelling for dynamic studies in power systems [2],[3],[4]. These research have had substantial contributions to create test simulation systems that represent real power systems.

Although both synchronous generators and load models are considered as main elements of any test system used to acquire a comprehensive understanding of the real power system behaviour [5], load modelling still remains as one of the most challenging tasks. The challenges rest in the high number of devices of which the load consists, as well as the plethora of characteristics of the loads. Therefore, most of the TSOs nowadays apply so called "aggregated load modelling" in their practices. The Nordic TSOs use ZIP load model structure to represent the load in the system. The ZIP load structure is one of the load structures that gives a good overview of the system load behaviour and is being used by TSOs for building their test systems. These test systems provide the environment that TSOs need for network planning and decision making purposes, owing to the flexibility ensured by these systems in testing and verifying different strategies that could be applicable in the real network [5].

1.1 Background of the project

This thesis work is being done in collaboration with the Nordic TSOs and ABB Power Consulting. The objective of the project is to acquire good knowledge of load modelling and its application to improve existing load models. These load models are used in software like PSS/E to simulate real networks. In this project, the load model is aggregated regardless of the load class and its composition at the evaluation point. Therefore, to develop a reliable model of the load, the load behaviour needs to be considered. This behaviour is significant when critical events occur in the real network. Effects of these events can be revealed in the measurement data supplied by the TSOs. Thus, the vast amount of measurements provided by

the TSOs could include voltage dips or frequency deviations that are helpful for load modelling purposes [5].

Load models can provide information about voltage and frequency dependency of the load, that can be represented by combining both polynomial and exponential expressions, whereas the coefficients determine the performance of the load model [6]. However, for the time being, there is lack of evidence and knowledge on how to identify the most suitable coefficients that are included in the model. Consequently, this project has been brought up by ABB Power Consulting and the Nordic TSOs in order to make further improvements on the present load model coefficients utilized in the existing test systems. Availability of data provided by the TSOs makes the measurement based approach more appropriate for this thesis work [2],[5],[7].

1.2 Objectives

The main goal of this thesis work is to obtain load model parameters that result in more accurate representation of the load. Also, the methodologies used for load modelling applications will be investigated to get a comprehensive understanding of load modelling and its behaviour. In this project, measurement-based approach will be employed to improve the currently used coefficients in the load model, with the aim of providing results that are sufficiently close to reality. Obtaining accurate results will provide an efficient support to the TSOs for future plans in terms of development and investments in the electric power system.

1.3 Problem description

Analyzing the measurements given by the TSO is the fundamental process in order to modify the existing coefficients of the load model. These measurements include the load response to events occurring on chosen evaluation points. Therefore, a vast amount of data will be analyzed to detect and verify the most interesting events resulting in voltage dips in the real network. Time of these events will be determined to observe the load response in active and reactive power. Subsequently, different curve-fitting techniques can be applied to obtain the new coefficients of the ZIP load model. These coefficients will be verified after conducting the simulation in PSS/E and analyzing the new load response. Furthermore, a comparison between the results of different coefficients sets will be investigated to provide valuable input for the understanding of the load response. Choosing suitable parameters for the load model is essential in power system simulations as they have significant impacts on the system's behaviour.

1.4 Limitations

The load model structure has been chosen in this thesis is the ZIP load model as it is mainly used and recommended for power flow and dynamic simulations [2]. For

the derivation of the ZIP load model parameters, two different techniques can be applied:

- Component-based (bottom-up) approach
- Measurement-based (top-down) approach

However, in the component-based approach, the load composition and characteristics of each electrical load are required. Therefore, this method tends to not be applicable due to the lack of knowledge of the dynamic behaviour assigned to the different load components. On the other hand, a vast amount of data representing the measurements at the selected evaluation points are supplied by the local DSOs. These data will make the measurement-based approach more suitable for this project.
Events that reflect the load responses are important to be specified in the given data. These events are mainly voltage or frequency events. In general, this thesis focuses on the voltage events represented by the voltage dips in the evaluation points. On the other hand, there are some aspects will not be covered in this thesis including:

- Actions that caused the voltage events.
- Selection criteria of the evaluations points.
- How the measurements were conducted.
- Frequency events are not considered in this study. Therefore, load frequency dependency of the load is not represented in the load model structure.

1.5 Previous work

With the increasing demand of electricity and the existing variety of power resources, today's power networks are expanding in all sides. This expansion is accompanied with different challenges in network operations in terms of generation, transmission, and distribution. Therefore, the need for implementing effective plans that ensure a reliable and economic behaviour of the system cannot be neglected. In general, the power system consists primarily of four parts: generation, transmission and sub-transmission, distribution and electrical loads [8]. Generating units such as nuclear power plants, thermal units, hydro power and wind turbines produce the electric power which is then distributed via transmission network to the sub-transmission network, and eventually, to the distribution network that delivers the power to the end consumers. Figure 1.1 gives an illustration of modern power system network as described by Vattenfall AB.

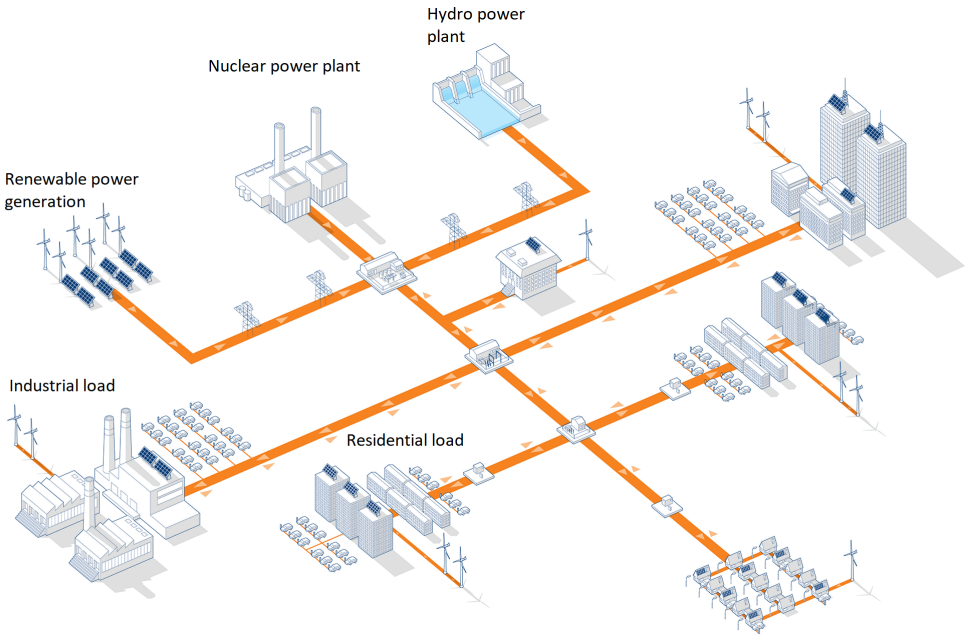

Figure 1.1: A schematic overview of a modern power system. Adopted from Vattenfall AB website.

For the operating and planing phase of such large networks, it is important to have models that represent the aforementioned components of the real power system. Thus, accurate modelling of generators, transmission lines and loads has been one of the main objectives of the TSOs. Amongst these elements, the load is considered the hardest part to be modelled due to its diversity and stochastic behaviour. Till a while ago, load modelling was not on the top of the priority list as the generators were for instance. Nowadays, acquiring an appropriate representation of the load is possible even if load modelling is completely different from generator or transmission modelling. The interest towards developing accurate load models started increasing after some critical accidents such as the voltage collapse in Sweden in 1983 and the major power outage that took place in North America in 1996 where 7.49 million customers were affected [9]. The inspection results revealed that the insufficient load models were the main reason behind these crucial events.

Consequently, significant efforts have been consistently undertaken by the Institution Of Electrical and Electronic Engineers (IEEE) in the years between 1992 and 1995. In 1992 IEEE published one paper which included basic description of load modelling, the importance of load modelling and what actions to take in purpose of dynamic studies in power systems. Another paper was published in 1995 contained a comprehensive literature list regarding load model representation consisting of tables of different load types as well as typical parameter data for the specific load

types [2],[3]. In addition to this, other relevant work has been published concerning load modelling and load aggregation as presented in [10] and [11] by the *Conseil International des Grands Réseaux Électriques* (CIGRE). In these publications more discussion about load modelling and the understanding of loads in power systems and the challenges faced in developing simple but realistic load models are performed.

Load models are divided into two main categories: static and dynamic models. In the dynamic load models, the previous and the current states of the voltage and the frequency are considered when modelling the load [12], whereas static load models are represented using time-invariant functions of the voltage and frequency. Therefore for any instant of time, load behaviour is determined as a function of the voltage and the frequency at that specific instant. Static load models are the dominant models adopted in load modelling processes and can be expressed in two different mathematical expressions: polynomial and exponential [13]. These polynomial and exponential static models are functions of voltage, and can also be functions of frequency by multiplying the mathematical expressions of these models by an exponential function of frequency whose exponent mimics the frequency dependency of the load's behaviour [14],[15]. Static load models are reasonable to use for studying the system response few seconds after a disturbance and such disturbances can be an outage or a trip of a line. For longer time periods, dynamic load models are required in order to obtain accurate load behaviour representation. A recently conducted survey revealed that 70% of the transmission system operators use static load models for stability studies of power systems [13].

1.6 Disposition

The structure of the thesis work is as follows. Chapter 2 introduces basic concepts and knowledge of power system load modelling and load aggregation. Chapter 3 presents the methodology of this thesis, i.e., the general steps to be carried out throughout this thesis in order to implement measurement-based approach. In chapter 4 the results of applied methodology are presented, followed up by result discussion in chapter 5. Finally, chapter 6 concludes the thesis work and presents proposed thoughts for future work.

2

Power system load modelling

2.1 Load modelling

In this chapter, the notion of load modelling and associated concepts such as the load aggregation are studied. The models used by the (TSO)s for static and dynamic studies are also presented. Additionally, the electrical loads of the power system and their classifications based on different characteristics are also discussed.

Load

In power systems, the load represents the amount of active and reactive power needed for operating electrical devices connected to the grid. Since the word load is a broad concept, it can be specified differently based on the given system and aspects of interest chosen for the study. In other words, the load could be the power consumed by a generator, non modeled components or the total power demand for the whole system. The mathematical expression of the load's apparent power is

$$S = P + jQ \tag{2.1}$$

where S, represents the apparent power in (VA), P, denotes the active power in (W) and Q is the reactive power in (VAr). P and Q are also expressed as

$$P = Scos(\theta) \tag{2.2}$$

$$Q = Ssin(\theta) \tag{2.3}$$

where θ is the displacement angle between the supply voltage and the load current at the load bus.
The displacement power factor can be obtained by using the displacement angle θ as

$$DPF = cos(\theta) \tag{2.4}$$

In the case of non-linear loads, the true power factor is affected by the harmonics introduced in the system and can be written as

$$PF = \frac{cos(\phi)}{1 + \sqrt{THD_i^2}} \tag{2.5}$$

where THD_i is the total harmonic distortion of the load current [16].

The harmonic distortion effect can be observed in the figure 2.1 where the vector diagram shows the harmonic distortion D, the displacement angle of the distortion ϕ and the fundamental apparent power $S1$ [17].

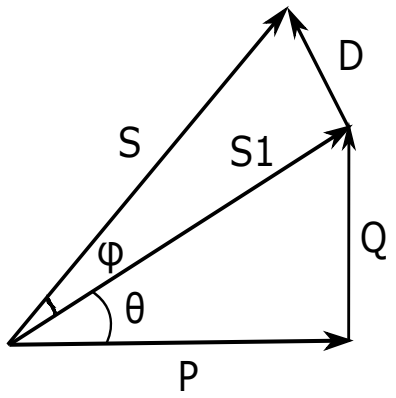

Figure 2.1: Representation of complex power in vector form including harmonic distortion. Figure adopted from [17].

Load characteristics

The load can be characterized in different ways- either by the power factor or by a set of coefficients in a load representing model. These coefficients determine the load response in active and reactive power to supply voltage or frequency variations.

Load component

Load component is an essential concept used for load modelling purposes in power systems. Load component represents the aggregation of all electrical equipment that are of similar type and nature such as lighting sources, motors or resistive loads like electrical heaters.

Load class

Load class is a general expression used to describe the nature of the customer or a cluster of customers consuming electrical energy in a geographical zone. The main categories under which loads can be classified are: industrial, commercial and residential.

Load composition

Load composition refers to the participation in percentages of the components that collectively form the load at a specific bus. The load composition can be obtained for

each evaluation point in the system and it varies between different evaluation points as every evaluation point could be taken for different load class and consequently different load components.

Load class mix

Load class mix has a similar definition of the load composition, but the difference between the two terms is that the load class mix refers to the participation in percentage of every load class in the total load of the system.

Load model

Load models are developed and built to study the effects caused by voltage or frequency variations on loads behaviour. The voltage and frequency dependency of the load can be expressed using mathematical equations. Thus, load models include different structures: polynomial, exponential or transfer function besides some other structures. However, it is desirable to have a non complex model that describes the different cases of load response.

Load aggregation

Load aggregation is regarded as an one of the most important approaches of load modelling. The importance of load aggregation appears in big complex systems where it is not feasible to individually model every device in the system. Therefore, the need for applying this approach increases in systems with a large number of devices. Load aggregation in power systems can be achieved in two different ways: by analytically aggregating the loads in the system or by identifying model parameters from the measurements conducted at specific points.

2.2 Static load model structure

As previously mentioned in section 1.5, the load's active and reactive power can be mathematically expressed as functions of the voltage U and frequency f as seen in (2.6) and (2.7).

$$P = f_1(U, f) \tag{2.6}$$

$$Q = f_2(U, f) \tag{2.7}$$

Most of the existing static load models are sufficient in order to observe the load response shortly after a disturbance in voltage or frequency. Thus, static load models are frequently used in dynamic operations according to [13].

2.2.1 Constant impedance load model

In this model, active and reactive power are represented as functions of square of the voltage magnitude as shown in Figure 2.2.

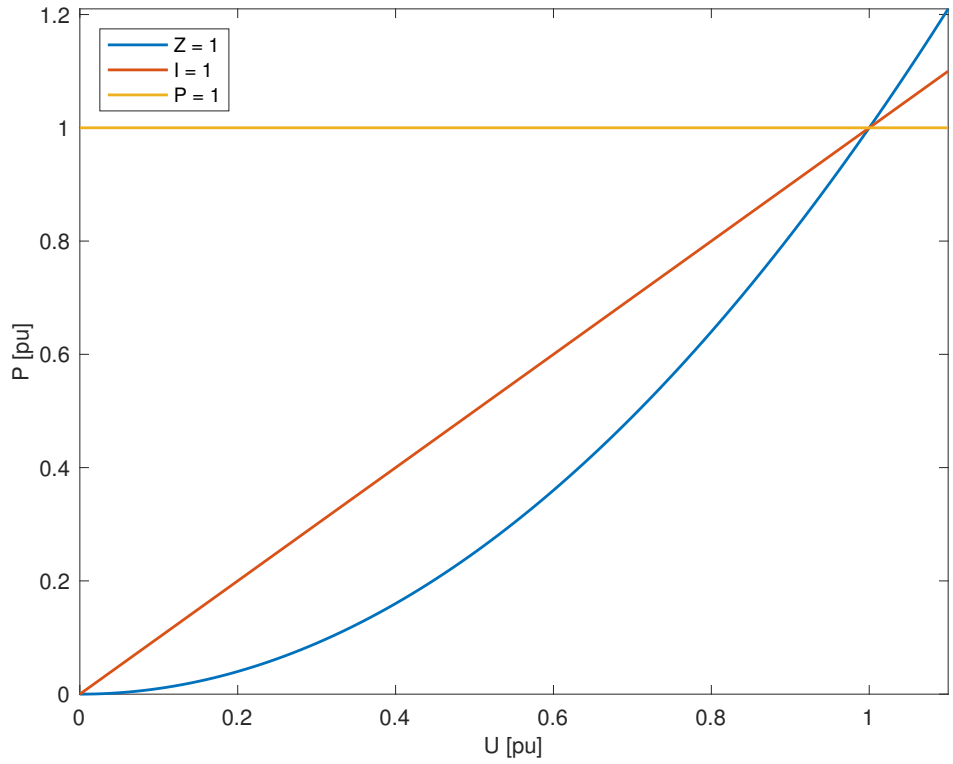

Figure 2.2: Load characteristics of the constant impedance, the constant current and the constant power. $Z = 1, I = 1, P = 1$ corresponds to the constant impedance, constant current and constant power, respectively.

2.2.2 Constant current load model

This model is characterized by a linear relation between the power and the voltage. This can also be seen in Figure 2.2.

2.2.3 Constant power load model

In this model, ss the name suggests, the power is always constant as shown in Figure 2.2, and most of the TSOs around the world use this load model load flow calculations [13].

2.2.4 Polynomial structure of load model

A wide range of load model structures have been proposed to reflect the physical load model or so called static load model. The polynomial load model is one of the most common load models used to represent the load. This load model is a combination of the constant impedance, constant current and constant power load characteristics shown in Figure 2.2. It is also associated with the term ZIP load model in literature.

The mathematical representation of the ZIP load model is given by equations

$$P(U) = P_0\Big(Z_p(\frac{U}{U_0})^2 + I_p(\frac{U}{U_0}) + P_p\Big) \tag{2.8}$$

$$Q(U) = Q_0\Big(Z_q(\frac{U}{U_0})^2 + I_q(\frac{U}{U_0}) + P_q\Big) \tag{2.9}$$

where Z_p, I_p, P_p, Z_q, I_q and P_q denote the proportional coefficients in percentage of the constant impedance, constant current and constant power in static active and reactive load. P_0, Q_0 and U_0 refer to the initial values of power and voltage measured in the system before the disturbance which can also be called the pre-disturbance operating conditions.

2.2.5 Exponential structure of load model

The exponential structure is another structure used in load modelling. This structure represents the load as a function of voltage as shown in equations

$$P(U) = P_0\Big(\frac{U}{U_0}\Big)^{n_p} \tag{2.10}$$

$$Q(U) = Q_0\Big(\frac{U}{U_0}\Big)^{n_q} \tag{2.11}$$

In (2.10) and (2.11), the exponents n_p and n_q are the model's parameters. These parameters determine the load representation as constant power, constant current or constant impedance models when they take the values 0,1 or 2 respectively. However, for some types of loads, these exponents can take other values which could be greater than 2 and less than 0 [3].

2.2.6 Frequency-dependent load model

As previously stated in Section 2.2, the static load model can also include the frequency dependency of the load. This can be represented by multiplying the polynomial or the exponential model with the term (2.12).

$$1 + k_{pf}(f - f_0) \tag{2.12}$$

Here, k_{pf} represents the sensitivity parameter of frequency. Furthermore, the parameters f and f_0 denote the system frequency and nominal frequency respectively. This frequency dependency is also included when other types of loads are modelled, for example, dynamic models of induction machine [18]. Recent observations show that if the difference between f and f_0 is small, and the value of k_{pf} is insignificant then this term can be neglected, but more research is needed to validate this effect [19].

3
Methodology

This chapter explains the methodology carried out in this thesis when using the measurement-based approach. This thesis deals predominantly with the polynomial ZIP load model as represented in section 2.2.4. Generally, load modelling comprises of two main procedures. The first is load model structure selection, followed by the second procedure of deriving model coefficients. These coefficients can be acquired either from previous studies (bottom-up) approach or obtained from field measurements (top-down) approach [10],[20]. Figure 3.1 presents the aforementioned procedures followed for developing the load model. Further details regarding the measurement-based approach and its application in this thesis are described more thoroughly in the coming sections.

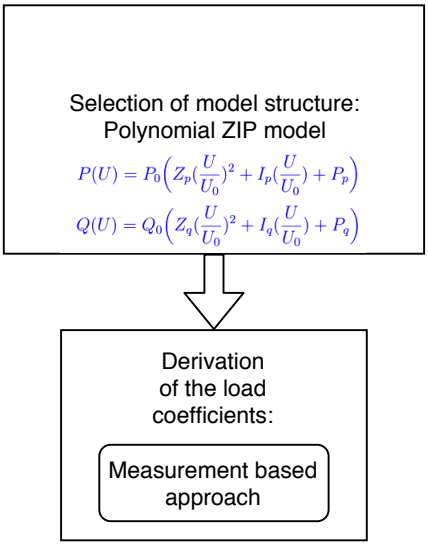

Figure 3.1: General process of the load modelling considering measurement-based approach [10].

3.1 Data processing

In this work, processing data obtained from some utilities is an essential procedure to start with in order to proceed with the measurement-based approach. Since, some parts of these measurements are given as raw data, the structured query language SQL is needed to access and manipulate these databases in order to make it more user friendly. After that, it is possible to obtain the data of interest and save them

in readable data sets using programming languages such as MATLAB and Python. These data sets can be later exported to the workspace in MATLAB where they become ready for further commands given by the user.

3.1.1 Data content

The data supplied by local DSOs in Sweden, Finland and Norway are sets of measurements taken at different geographical locations. A number of evaluation points have been selected to take measurements. These measurements include signals of voltage, active and reactive power taken every second for different time scales that vary from few days to a whole month. Therefore, some of these data sets are extremely large and require particular ways of handling. In the measurement based approach, the main focus is to deeply analyze these signals in order to have a comprehensive understanding of the load behaviour.

3.2 Measurement-based load modelling

In general, measurement-based approach can be seen as a 'system identification' problem. In other words, it is a curve-fitting task where the method uses measurements that reflects the dynamic behaviour of the electrical load under an event in the system. Using these measurements and fitting the data to the estimated model structure results in obtaining the coefficients of the model by optimizing an objective function. Basically, the optimization is performed by using parameter identification and curve-fitting techniques to minimize the error between the real system and the estimated model. In order to achieve these objectives, a closer look has been undertaken in following papers [10],[11],[19],[21],[22] and [23].

3.2.1 Curve-fitting algorithms

Regression analysis or so called curve-fitting algorithms are used to derive the load model coefficients. The principle of curve-fitting depends on finding the best line or curve that fits a series of data points and that can be achieved using different techniques. Curve-fitting algorithms can be divided into three categories: Least squares curve-fitting, non linear curve fitting and smoothing curve-fitting, which will be explained in subsequent sections.

3.2.1.1 Least squares curve-fitting

Least square is a popular method used to minimize the square of the error between measurements and curves obtained after applying an optimization process [24]. Comparing to other methods, least squares curve fitting is relatively simple and easy to understand. On the other hand, the drawback of this method is represented in its sensitivity to data outliers, that are points which are far from the rest of the data.

3.2.1.2 Non linear curve-fitting

Non linear curve-fitting is considered as an effective alternative to linear curve fitting due to the flexibility it ensures. This method tries to find the best fit of model to the data, eventually acquring the best values of parameters in this model [25].

3.2.1.3 Smooth curve-fitting

Here, in this type of curve-fitting, the smoothing curve fits are different from the previous two types of curve-fitting, as this type does not apply any equation to obtain the resulting curve. In other words, it is not possible to represent the curve using a single equation [26]. Examples of smoothing curve fits are: Smooth, Interpolate, Weighted and Cubic Spline [27], [28]. these different smooth fits apply different technique to obtain the curve wanted.

3.2.2 Pros and cons of measurement-based method

The main advantage of applying the measurement based approach is that we do not need to consider the information regarding load composition, class mix of the load or characteristics assigned to every load component. In this approach, all of these factors are aggregated together and coefficients of the load model are obtained from the measurements. The other important advantage of the measurement-based approach is represented in the possibility of applying it at load busses with large number of different loads [29]. On the other hand, the measurement based approach tends to be more stable and gives reliable results at higher voltage levels where there are less load variations unlike the lower voltage levels where the imbalance in load can be significantly noticeable [30]. However, the drawback of the measurement-based approach is that it can generate different set of coefficients that give acceptable results.

3.3 Model coefficients identification

This section provides a brief explanation of the two algorithms used for deriving the load model parameters, the Genetic Algorithm (GA) and Particle Swarm Optimization (PSO). Furthermore, the procedures followed during the implementation of these algorithms are also described including the selection of the initial conditions and the objective functions and constraints specified for the optimization problem.

3.3.1 Genetic algorithm

Finding the ZIP load model coefficients represents the core point of interest in this work. Therefore, different algorithms can be applied on the available data to obtain the ZIP loads parameters Z_p, I_p, P_p, Z_q, I_q and P_q. Genetic Algorithm (GA) is one algorithm that is widely used in load modelling and it has been selected in this thesis. GA application starts with arbitrarily setting a number of so called initial populations or in other words initial possible solutions. Then, based on the evaluation applied to the fitness function of every solution, the solutions will be

ranked [31], [32]. Subsequently, the fitness function optimization phase starts with developing the solutions using different operations such as crossover and mutation. Eventually, at the end of the optimization, a set of optimal solutions will be acquired. This process will repeat for a certain number of iterations until the termination criterion is satisfied. This algorithm is inspired by the process of natural selection of the evolutionary concept [31]. In general, population size needs to be defined for solving the optimization problem. Moreover, it is heavily dependant on the problem itself and can usually contain plenty of solutions.

In this thesis, the population number is chosen to be 150 and the evolutionary process is selected as mutation. Also, the other GA options such as, number of iterations and the fault tolerance of the function were set to be 800 and 10^{-45}, respectively.

The optimization problem solved for the GA algorithm and its objective function and boundaries are found as.

$$\begin{aligned} \min_{Z_p, I_p, P_p} \quad & \frac{1}{N}\sum_{n=1}^{N}(P_n - \hat{P}_n)^2 \\ \text{Subject to:} \quad & Z_p + I_p + P_p - 1 = 0 \\ & 0 \geq Z_p \geq 1 \\ & 0 \geq I_p \geq 1 \\ & 0 \geq P_p \geq 1 \end{aligned} \tag{3.1}$$

As presented in (3.1), the objective in this case is to minimize the square of the error between the measured power and the load model power at every sample $\hat{P}_n$, and N is the number of samples. The load model power or estimated power, $\hat{P}_n$, is expressed as.

$$\hat{P}_n = P_0\Big(Z_p(\frac{U_n}{U_0})^2 + I_p(\frac{U_n}{U_0}) + P_p\Big) \tag{3.2}$$

Here, P_0 and U_0 are associated with the initial values of power and RMS voltage before the disturbance. Furthermore, U_n denotes the n:th measured RMS voltage obtained from the given data.

In order to obtain the coefficients for reactive power a similar set up is used allowing the coefficients in this case to have negative values. The equations used for coefficients derivation are expressed in (3.3) and (3.4).

$$\begin{aligned} \min_{Z_q, I_q, P_q} \quad & \frac{1}{N}\sum_{n=1}^{N}(Q_n - \hat{Q}_n)^2 \\ \text{Subject to:} \quad & Z_q + I_q + P_q - 1 = 0 \end{aligned} \tag{3.3}$$

$$\hat{Q}_n = Q_0\Big(Z_q(\frac{U_n}{U_0})^2 + I_q(\frac{U_n}{U_0}) + P_q\Big) \tag{3.4}$$

Additionally, as mentioned in section 2.2.5, another structure, the exponential structure, can be used for load modelling purposes. This structure has the following parameters n_p and n_q as shown in equations (2.10) and (2.11) used for the optimization when applying GA algorithm on the given data.

3.3.2 Particle swarm optimization

The second optimization technique used in this thesis is the Particle Swarm Optimization (PSO). The interesting fact of this algorithm is that it was inspired from nature [33], as in the biological systems and it imitates the states of bird and fish pools [34]. In general, PSO mechanism depend on randomly finding a group of particles that represent possible candidates for the optimization problem solution. Velocity of each particle will be consistently changed and is accelerated to reach the 'best' location. As other population-based methods, this algorithm starts by randomly choosing initial variables for position and velocity of particles. Then, the procedure continues with computation of the objective function, which in this case is the same as presented in (3.1). This process continues until certain termination conditions are satisfied such as maximum number of iterations which is pre-defined in the algorithm. Furthermore, according to [34], the velocity and position vectors are updated in accordance with,

$$v_{k+1}^i = wv_k^i + c_1 rand(\frac{p^i - x_k^i}{\Delta t}) + c_2 rand(\frac{p_k^g - x_k^i}{\Delta t}) \tag{3.5}$$

$$x_{k+1}^i = x_k^i + v_{k+1}^i \Delta t \tag{3.6}$$

where, w, c_1 and c_2 are constants, w is the inertia factor and can take values between 0.4 and 1.4, and c_1,c_2, are normally selected as 2 [35].

In this simulation, the initialization of the variables are adopted from [34], where w is varying from 0.4 to 0.9 and the maximum number of iterations are found to be 2000, whereas the population size is selected as 150. Eventually, the algorithm will stop when the change of 'best' particle are less than 10^{-4} over the last 500 iterations.

4
Results

As mentioned before in chapter 3, the measurement based approach has been chosen to find the parameters of the load model whose structure has been selected to be the ZIP model structure. This chapter presents the case studies performed in this thesis, where the methodologies described in chapter 3 are applied to obtain the model coefficients. The study has been structured based on the season of the year and the day if it is a working day or a weekend. The results in the subsequent sections are presented based on seasons of the year for several datasets. The mean absolute percentage error is chosen as the metric to present accuracy of the load model.

In order to start with the study the data must be made readable and ready to process as it represents the base on which this study is conducted. Therefore, in some cases, the first task is to process the data provided to get it ready for further work as the given data can be raw and its content can not be reached directly.

In this section, the study has been conducted for two evaluation points. The data from these two points were processed and the fore-mentioned algorithms have been applied in order to obtain the ZIP load coefficients. In addition, the study has also been applied for other evaluation points and the results will be presented in the Appendix section.

For the evaluation point 1, the case of selecting the exponential load model was also considered and the parameters together with the error assigned to the exponential load model are presented in the subsequent sections.

4.1 Season-based study for evaluation point 1

It is known that behaviour of the load and the load demand in the power system vary significantly between the seasons. This study will help TSOs to acquire a comprehensive understanding of the load behaviour during different seasons of the year taking into account whether an event occurs in the working days or weekends and if the event has occurred during the day time or the night time. Moreover, this can give us flexibility in choosing the suitable sets of parameters in the test models for planning studies. Here, the data provided from evaluation point 1 did not require any data processing as it was already readable.

Winter

Based on the data supplied by the evaluation point 1, following results for the load model coefficients are shown in table 4.1. The mean absolute percentage error corresponding to the derived model are obtained for Winter 2018 are given in table 4.2. Moreover, figures 4.1 and 4.2 show the load performance after applying curve-fitting techniques with the original signal, which refers to the measured signal.

Table 4.1: ZIP load model coefficients obtained using GA and PSO algorithms for Winter.

	Algorithm	$\mathbf{Z_p}$	$\mathbf{I_p}$	$\mathbf{P_p}$	$\mathbf{Z_q}$	$\mathbf{I_q}$	$\mathbf{P_q}$
Dec							
	GA	0.9925	0.0085	0	-1.4439	0.0203	2.4236
	PSO	1	0	0	3.5816	1.5839	-4.2538
Jan							
	GA	0.3930	0.5137	0.0932	0.0001	0.0047	0.9942
	PSO	0.4841	0.5145	0	0.9054	10.0000	-10.0000
Feb							
	GA	0.1984	0.4868	0.3148	-3.2649	0.8754	3.3894
	PSO	0	0.9991	0	4.1227	3.4511	-6.7113

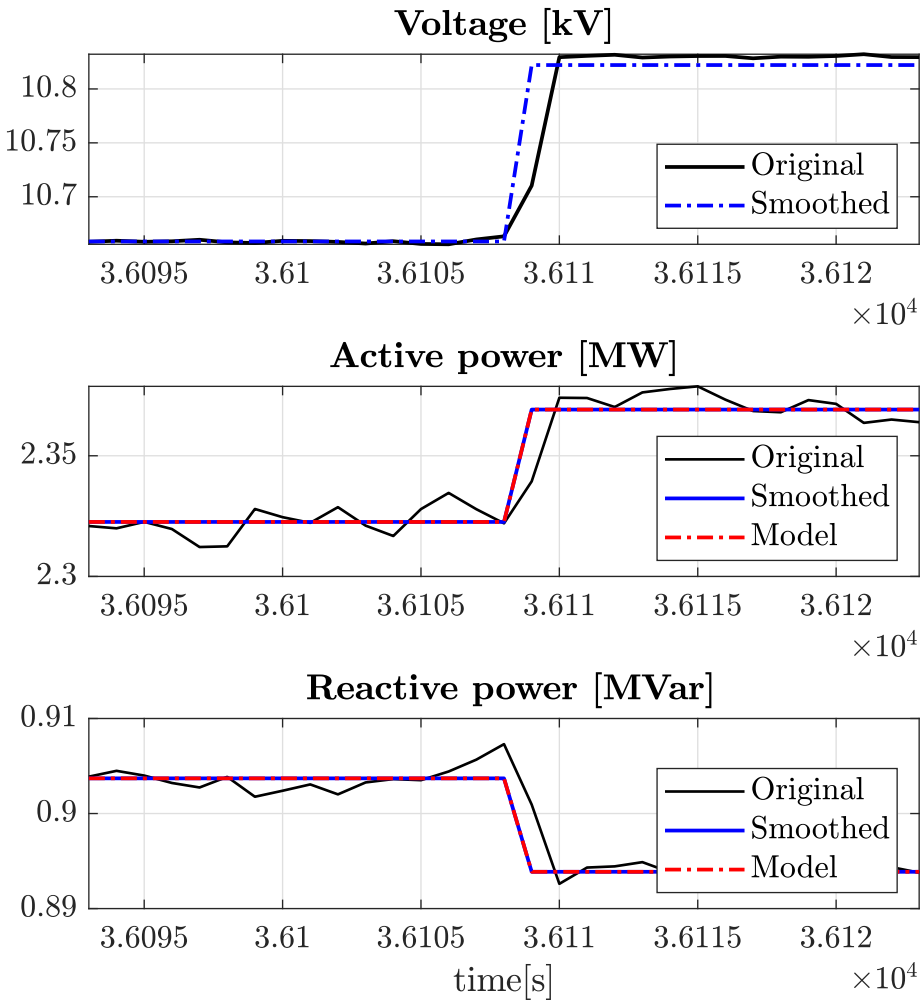

Figure 4.1: Results of measurement based approach applying GA algorithm.The black signal corresponds to original signal obtained from the measurements. The signal in blue represents the mean of the original signal before and after the disturbance. The red signal corresponds to the fitted ZIP load model with the parameters obtained for January in table 4.1.

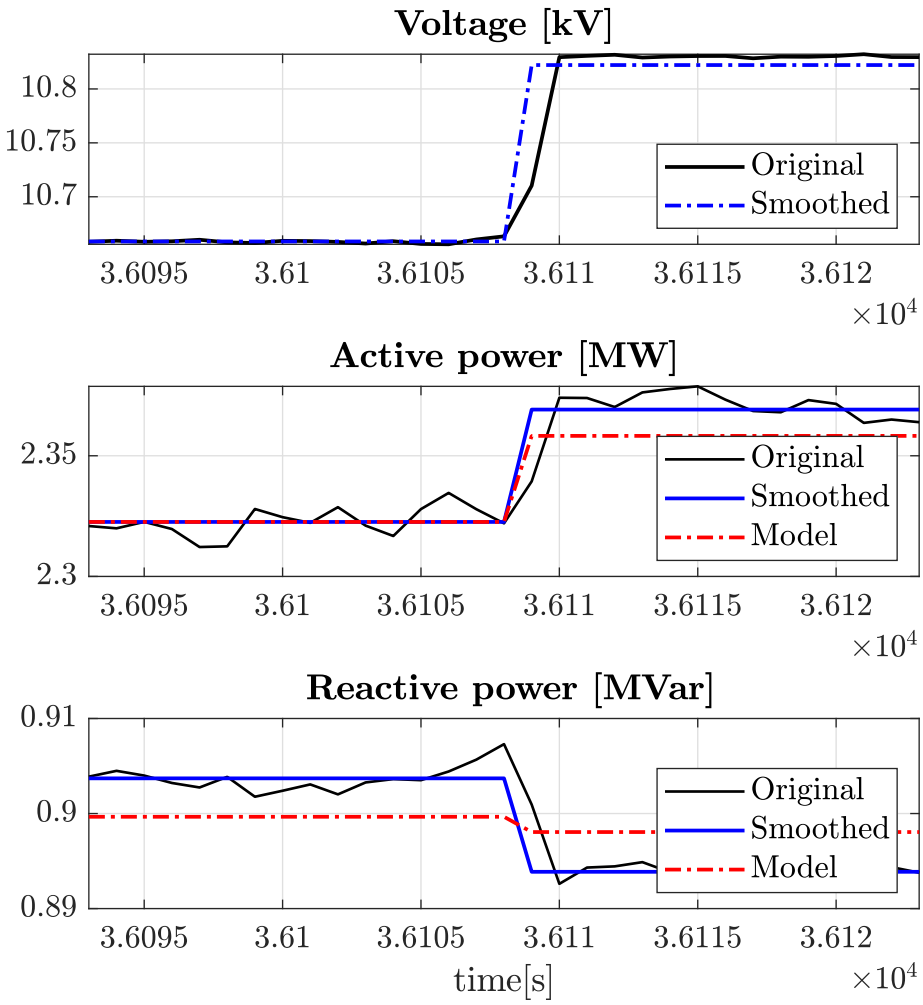

Figure 4.2: Results of measurement based approach applying PSO algorithm. The black signal corresponds to original signal obtained from the measurements. The signal in blue represents the mean of the original signal before and after the disturbance. The red signal corresponds to the fitted ZIP load model with the parameters obtained for January in table 4.1.

The mean absolute percentage error between the load model and original signal are calculated for December, January and February, respectively and shown in table 4.2. It can be observed that for the case of active power, the differences in percentage between the derived model and the real measurements are not that significant for the two algorithms. On the other hand, for the reactive power, the mean absolute percentage errors in December and January resulted after applying the algorithms are more significant compared to the errors in the active power for the relative months. Based on the results obtained after applying two different algorithms, GA can be considered to have better performance than PSO regarding the curve fitting purposes.

Table 4.2: The mean absolute percentage error for active and reactive power.

	GA	**PSO**
Dec		
P	0.8578%	0.8547%
Q	1.1813%	2.9600%
Jan		
P	0.2291%	0.3798%
Q	0.1264%	1.3640%
Feb		
P	0.5657%	0.5864%
Q	4.8418%	4.6277%

A closer look into the results reveals big variations in the values of the ZIP parameters. These variations in values of ZIP coefficients between the different months depends on whether the voltage event has occurred in a weekend as in the case of December, or if the events have occurred in working days as in the cases of January and February. For the working days in winter, after applying the GA algorithm on account of its smaller MAE, the coefficients are chosen as shown in the table 4.3.

Table 4.3: Range of obtained load model coefficients for working days in Winter.

$\mathbf{Z_p}$	$\mathbf{I_p}$	$\mathbf{P_p}$
(0.1984 - 0.3930)	(0.4868 - 0.5137)	(0.0932 - 0.3138)
$\mathbf{Z_q}$	$\mathbf{I_q}$	$\mathbf{P_q}$
(-3.2649 - 0)	(0.0047 - 0.8754)	(0.9942 - 3.3894)

Spring

Similarly, the algorithms have been applied on data given in dataset 1 that correspond to the months in spring season. The following table 4.4 shows the sets of coefficients obtained for each month in spring 2018. Furthermore, figures 4.3 and 4.4 present the results after applying the curve fitting algorithms, GA and PSO on the data corresponding to March 2018.

Table 4.4: ZIP load model coefficients obtained using GA and PSO algorithms for Spring.

	Algorithm	$\mathbf{Z_p}$	$\mathbf{I_p}$	$\mathbf{P_p}$	$\mathbf{Z_q}$	$\mathbf{I_q}$	$\mathbf{P_q}$
Mar							
	GA	0.6101	0.2897	0.1002	-7.7830	3.4523	5.3297
	PSO	1	0	0	5.9065	1.9036	-7.1110
Apr							
	GA	0.0001	0.1158	0.8832	-0.4835	-0.1248	1.6083
	PSO	0	0	1	7.9295	-1.4073	-5.6353
May							
	GA	0.1709	0.4055	0.4236	-0.1786	-0.0844	1.2629
	PSO	0	1	0	6.7770	-2.8048	-3.0627

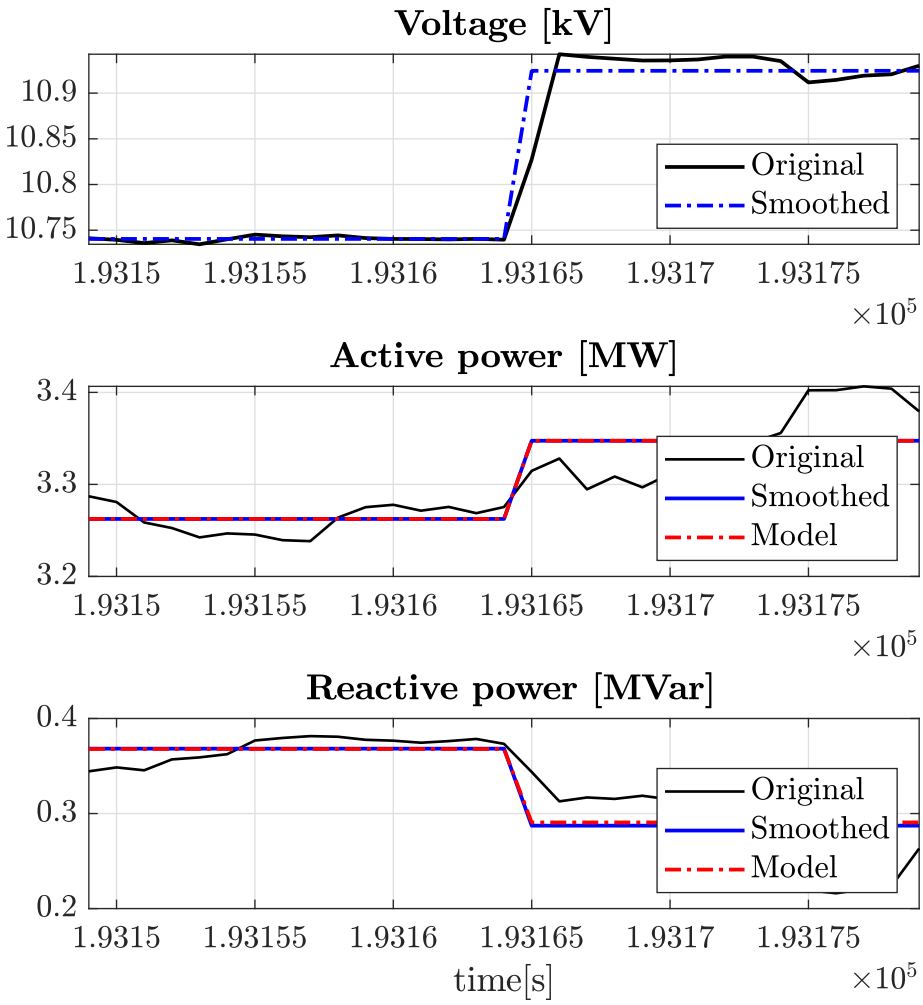

Figure 4.3: Results of measurement based approach applying GA algorithm. The black signal corresponds to original signal obtained from the measurements. The signal in blue represents the mean of the original signal before and after the disturbance. The red signal corresponds to the fitted ZIP load model with the parameters obtained for March in table 4.4.

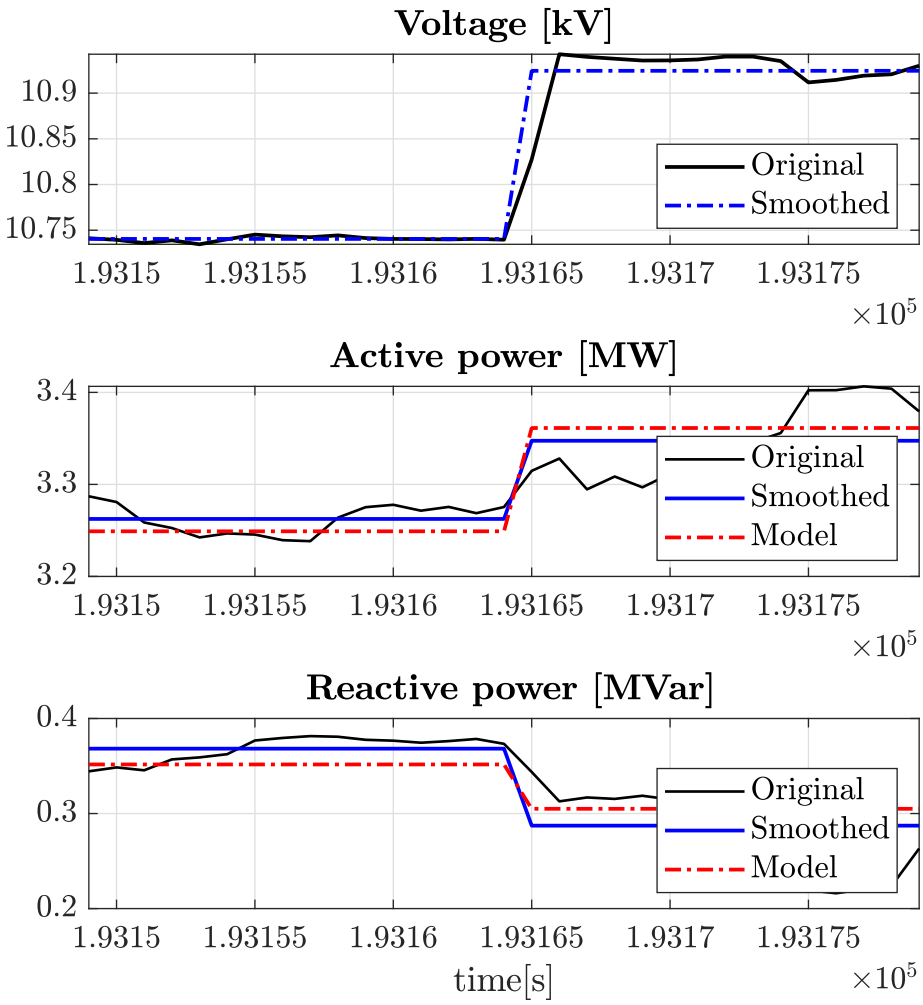

Figure 4.4: Results of measurement based approach applying PSO algorithm. The black signal corresponds to original signal obtained from the measurements. The signal in blue represents the mean of the original signal before and after the disturbance. The red signal corresponds to the fitted ZIP load model with the parameters obtained for March in table 4.4.

As before, the mean absolute percentage errors have been calculated in order to check the effectiveness of applying GA and PSO algorithms. The signals correspond to the load model and the real measurements for March, April and May as shown in table 4.5. It can be observed that for the case of active power, the differences in percentage between the derived model and the real measurements are not that significant for the two algorithms. On the other hand, for the reactive power, the mean absolute percentage errors in April and May after applying the algorithms are more significant as compared to the errors in the active power for the relative months. Thus, based on the results obtained after applying two different algorithms, GA can be considered to have better performance for curve-fitting purposes in this case than PSO.

Table 4.5: The mean absolute percentage error for active and reactive power.

	GA	PSO
Mar		
P	0.7508%	0.8714%
Q	6.6311%	7.1697%
Apr		
P	0.6949%	0.6948%
Q	0.5148%	2.2269%
May		
P	0.4685%	0.5138%
Q	0.3767%	1.0146%

The differences in values of the coefficients in table 4.4, are related to the time at which the event has occurred. As all the events in spring occurred on working days, one of them happened during the night time in April when the load demand is low. The other two events that occurred in March and may have occurred during the peak hours of the day. Therefore, the following range is obtained for the working days during the day time in the spring as found in table 4.6.

Table 4.6: Range of obtained load model coefficients for working days during the day time in spring.

$\mathbf{Z_p}$	$\mathbf{I_p}$	$\mathbf{P_p}$
(0.1709 - 0.6101)	(0.2897 - 0.4055)	(0.1002 - 0.4236)
$\mathbf{Z_q}$	$\mathbf{I_q}$	$\mathbf{P_q}$
(-7.7830 - -0.1786)	(-0.0844 - 3.4523)	(1.2629 - 5.3297)

Summer

Continuing with the results, the same procedure was carried out for summer 2018. Table 4.7 shows the obtained parameters after employing the same algorithms. Also, the results of the mean absolute percentage errors have been calculated and shown in table 4.8.

Figures 4.5 and 4.6 are also showing the results of applying GA and PSO algorithms respectively on the data given for June 2018. Here, there are small differences in the values of parameters obtained for June and July as the events in these months occurred over the weekend unlike events in August, that occured during the day.

Table 4.7: ZIP load model coefficients obtained using GA and PSO algorithms for Summer.

	Algorithm	$\mathbf{Z_p}$	$\mathbf{I_p}$	$\mathbf{P_p}$	$\mathbf{Z_q}$	$\mathbf{I_q}$	$\mathbf{P_q}$
Jun							
	GA	0.4781	0.3590	0.1629	4.7351	2.8712	-6.6063
	PSO	0.6074	0.3901	0	6.9217	4.0000	-10.0000
Jul							
	GA	0.4135	0.4894	0.0971	6.7013	-1.0954	-4.6058
	PSO	0.5506	0.4473	0	10.0000	0.9260	-10.0000
Aug							
	GA	0	0	1	4.2223	1.1825	-4.4048
	PSO	0	0	1	3.5352	3.7414	-6.6311

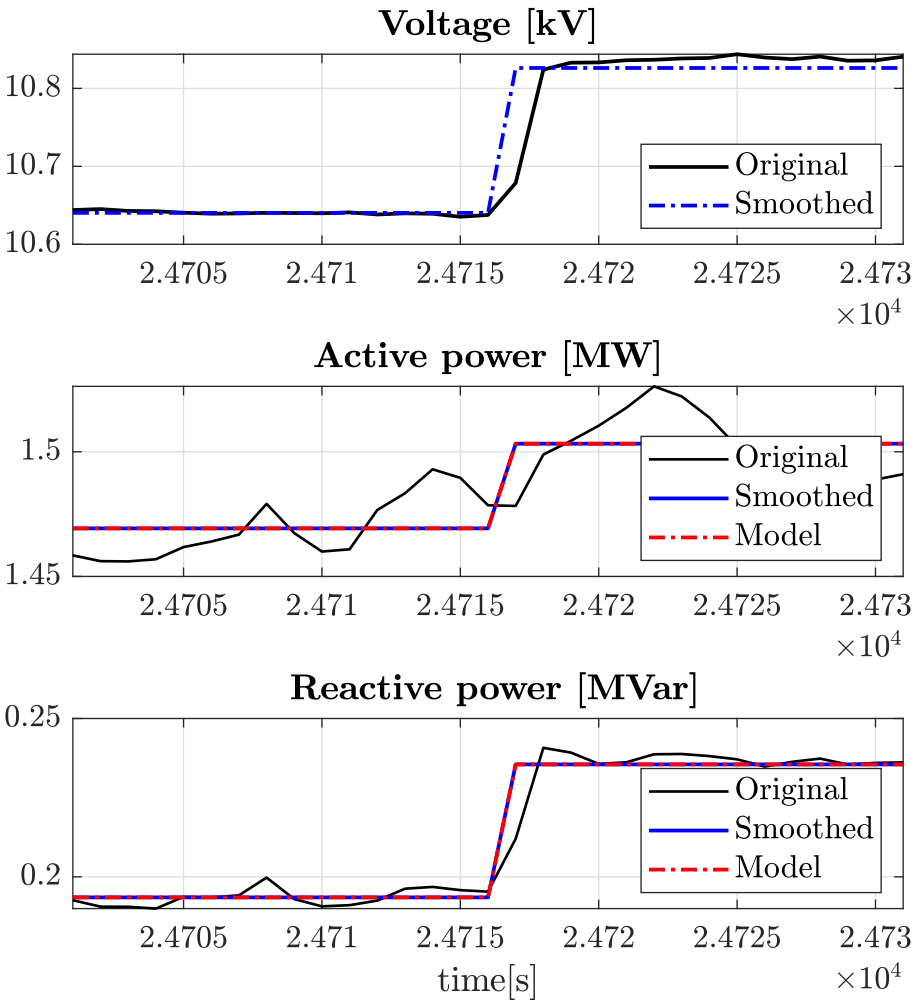

Figure 4.5: Results of measurement based approach applying GA algorithm. The black signal corresponds to original signal obtained from the measurements. The signal in blue represents the mean of the original signal before and after the event. The red signal corresponds to the fitted ZIP load model with the parameters obtained for July in table 4.7.

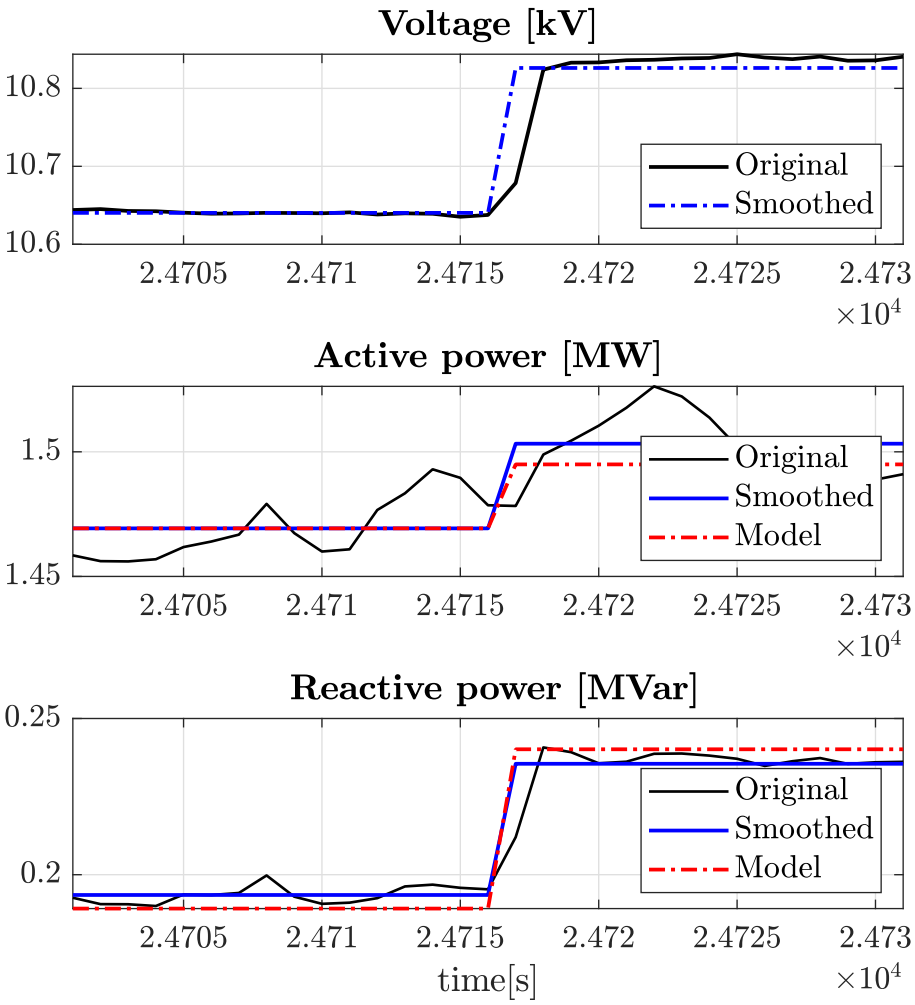

Figure 4.6: Results of measurement based approach applying PSO algorithm. The black signal corresponds to original signal obtained from the measurements. The signal in blue represents the mean of the original signal before and after the event. The red signal corresponds to the fitted ZIP load model with the parameters obtained for July in table 4.7.

As can be seen in table 4.8, the results of the mean absolute percentage error reveals that for the GA algorithm, similar results were obtained for June and July. In case of PSO, the same percentage error is observed in the active power for June and July. The percentage error in June and August for PSO algorithm appears to be the same.

Table 4.8: The mean absolute percentage error for active and reactive power.

	GA	PSO
Jun		
P	0.7042%	0.7834%
Q	1.3805%	3.2067%
Jul		
P	0.7042%	0.7834%
Q	1.3805%	2.3415%
Aug		
P	0.4945%	0.7834%
Q	1.0577%	3.2067%

Here, there are small differences in the values of parameters obtained for June and July as shown in table 4.9. The events in these months occurred over the weekend, unlike August where the event was on a working day.

Table 4.9: Range of obtained load model coefficients for weekends in Summer.

$\mathbf{Z_p}$	$\mathbf{I_p}$	$\mathbf{P_p}$
(0.4135 - 0.4781)	(0.3590 - 0.4894)	(0.0971 - 0.1629)
$\mathbf{Z_q}$	$\mathbf{I_q}$	$\mathbf{P_q}$
(4.7351 - 6.7013)	(-1.0954 - 2.8712)	(-6.6063 - -4.6058)

Autumn

The same procedure has been followed to get the coefficients in Autumn and results are shown in table 4.10.

Table 4.10: ZIP load model coefficients obtained using GA and PSO algorithms for Autumn.

	Algorithm	Z_p	I_p	P_p	Z_q	I_q	P_q
Sep							
	GA	0.2356	0.5549	0.2095	3.0633	0.3194	-2.3826
	PSO	0	1	0	6.8052	4.1122	-10.0000
Oct							
	GA	0.2561	0.4393	0.3046	0.9999	0.0010	0
	PSO	0	1	0	7.9593	-0.7476	-6.2896
Nov							
	GA	0.0255	0.9158	0.0587	0.9999	0.0011	0
	PSO	0	1	0	10.0000	-0.7106	-8.3898

October is the month selected to present the results of applying the same curve fitting algorithms. The results of applying these algorithms are shown in figures 4.7 and 4.8.

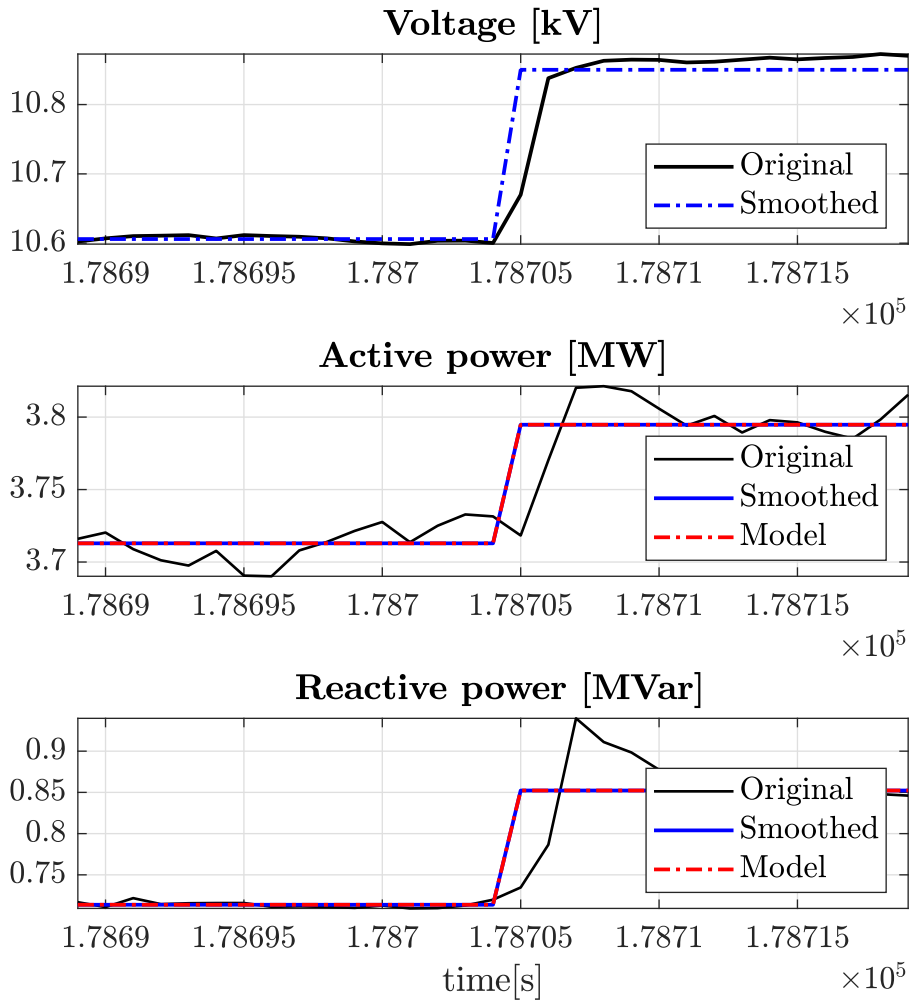

Figure 4.7: Results of measurement based approach applying GA algorithm. The black signal corresponds to original signal obtained from the measurements. The signal in blue represents the mean of the original signal pre and after the disturbance. The red signal corresponds to the fitted ZIP load model with the parameters obtained for October in table 4.10.

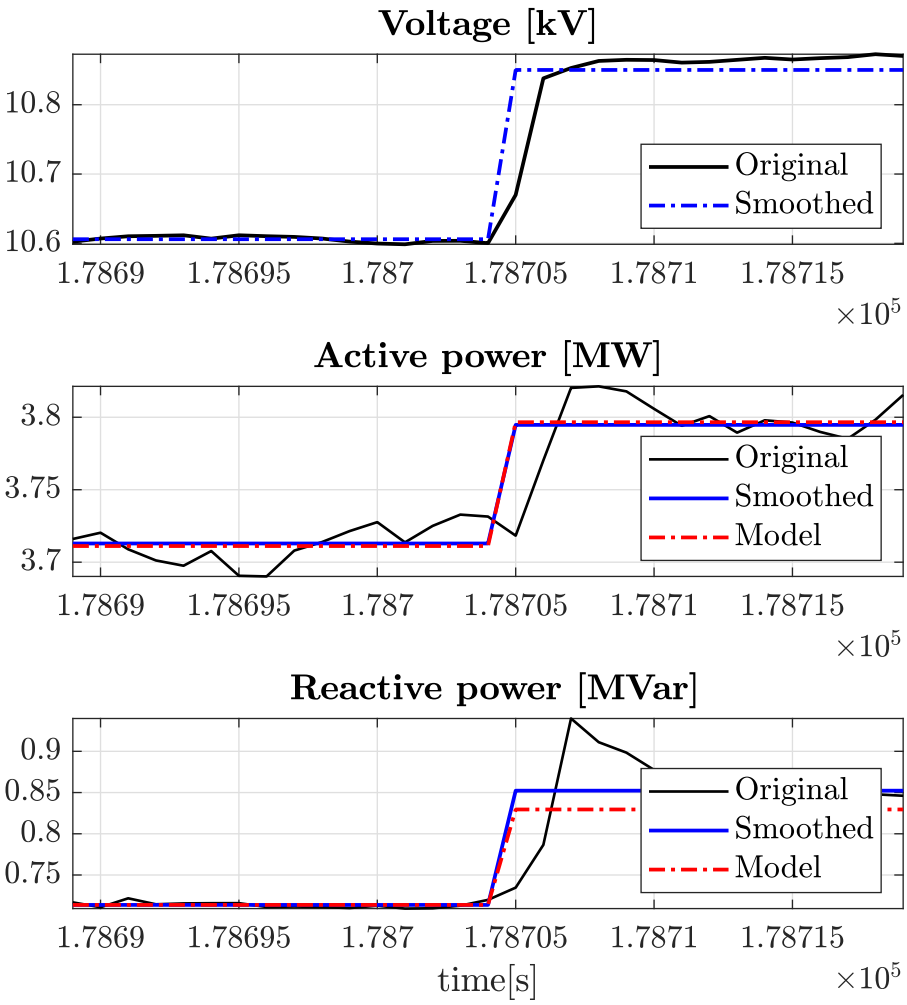

Figure 4.8: Results of measurement based approach applying PSO algorithm. The black signal corresponds to original signal obtained from the measurements. The signal in blue represents the mean of the original signal pre and after the disturbance. The red signal corresponds to the fitted ZIP load model with the parameters obtained for October in table 4.10.

As done previously, the mean absolute percentage errors have been calculated in order to observe the performance of the load after applying GA and PSO algorithms. As can be seen in table 4.11, the obtained results are close to each other, which reveals that the effectiveness of these two algorithms yields a good curve-fitting.

Table 4.11: The mean absolute percentage error for active and reactive power.

	GA	PSO
Sep		
P	0.2702%	0.2752%
Q	0.3773%	1.2209%
Oct		
P	0.3606%	0.3123%
Q	3.3320%	3.0084%
Nov		
P	0.3448%	0.3429%
Q	3.9126%	3.2305%

As all the events have occurred during the working days in Autumn in the day time, the following table 4.12 gives a range of values can be chosen for the model parameters:

Table 4.12: Range of obtained load model coefficients for working days during the day time in Autumn.

$\mathbf{Z_p}$	$\mathbf{I_p}$	$\mathbf{P_p}$
(0.0255 - 0.2561)	(0.4393 - 0.9158)	(0.0587 - 0.3046)
$\mathbf{Z_q}$	$\mathbf{I_q}$	$\mathbf{P_q}$
(appr 1 - 3.0633)	(0.0010 - 0.3194)	(-2.3826 - 0)

In general, all the ranges given in the previous section are for the GA algorithm as it achieved better performance, which was observed in the mean absolute percentage errors for the active and reactive power.

4.1.1 Results of exponential model parameters

In this section, the obtained parameters of the exponential load model with the GA algorithm are shown in table 4.13. Similarly, n_p was constrained to take values between 0 and 2, while n_q was not constrained. The following results are acquired for the whole year at evaluation point 1. It can be noticed that for the months September,October and November, the load parameter n_p takes values close to 1, which can be interpreted as constant current load. For March and December, n_p is approximately 2, which corresponds to a constant impedance load. On the other hand, when n_p is close to zero that means that the load can be considered as constant power load.

Table 4.13: Exponential load model coefficients obtained using GA for evaluation point 1.

	Algorithm	$\mathbf{n_p}$	$\mathbf{n_q}$
Jan			
	GA	1.3028	-0.7180
Feb			
	GA	0.8877	-6.0318
Mar			
	GA	1.5136	-14.6296
Apr			
	GA	-0.1216	-1.1165
May			
	GA	0.7515	-0.4496
Jun			
	GA	1.3199	11.3418
Jul			
	GA	1.3200	11.3419
Aug			
	GA	-0.0728	9.1062
Sep			
	GA	1.0293	6.2419
Oct			
	GA	0.9578	7.7966
Nov			
	GA	0.9674	6.3031
Dec			
	GA	2.4564	-2.9793

In table 4.14, the resulting error between the obtained exponential load model and measurements can also be observed. The reason behind the big error found in March is possibly due to the small detected step in reactive power.

Table 4.14: The mean absolute percentage error for active and reactive power.

	GA
Jan	
P	0.2291%
Q	0.1264%
Feb	
P	0.5657%
Q	4.8418%
Mar	
P	0.7508%
Q	46.7672%
Apr	
P	0.6814%
Q	0.5148%
May	
P	0.4685 %
Q	0.3768%
Jun	
P	0.7042%
Q	1.3806%
Jul	
P	0.7042%
Q	1.3805%
Aug	
P	0.4945%
Q	1.4577%
Sep	
P	0.2702%
Q	0.3773%
Oct	
P	0.3606%
Q	2.2864%
Nov	
P	0.3448%
Q	1.1695%
Dec	
P	0.7924%
Q	1.1813%

4.2 Season-based study for evaluation point 2

In this section, the study is repeated with the data provided from evaluation point 2. The study and the results obtained have been structured in the same manner as in section 4.1. Also, at the end of this section, sets of parameters will be provided for future planning studies.

Winter

Based on its acceptable performance in the case study for evaluation point 1, GA has been selected again in the case study of evaluation point 2 for curve-fitting purposes. Also, PSO algorithm was used as it gave reasonable results for the active power part of the load.

Unlike the data provided in the case study of the evaluation point 1, the data in this case study needed to be processed as it was raw. However, different software were used to restore the data and get into a more friendly use environment to visualize its contents of current, voltage and power measurements and store the time intervals of interest and its corresponding data. The load model coefficients obtained after implementing GA and PSO algorithms are presented in table 4.15 and the corresponding results are given in figures 4.9 and 4.10. Also, the mean absolute percentage errors have been calculated in table 4.16 for the purpose of observing accuracy of the load model is against the real physical system. Again, a closer look through table 4.16 will prove that GA algorithm gives more accurate results than PSO algorithm based on the mean absolute error resulted after applying the two algorithms.

Table 4.15: ZIP load model coefficients obtained using GA and PSO algorithms for Winter.

	Algorithm	$\mathbf{Z_p}$	$\mathbf{I_p}$	$\mathbf{P_p}$	$\mathbf{Z_q}$	$\mathbf{I_q}$	$\mathbf{P_q}$
Dec							
	GA	0.0165	0.0902	0.8933	1.5499	1.7509	-2.3008
	PSO	0	0	1	-0.0609	3.8046	-5.0000
Jan							
	GA	0	0	1	-0.0274	1.6684	-0.6410
	PSO	0	0	1	-0.0623	3.8503	-4.9896
Feb							
	GA	0.0009	0.0420	0.9571	1.9410	1.0057	-1.9467
	PSO	0	0	1	4.3357	1.2908	-4.6490

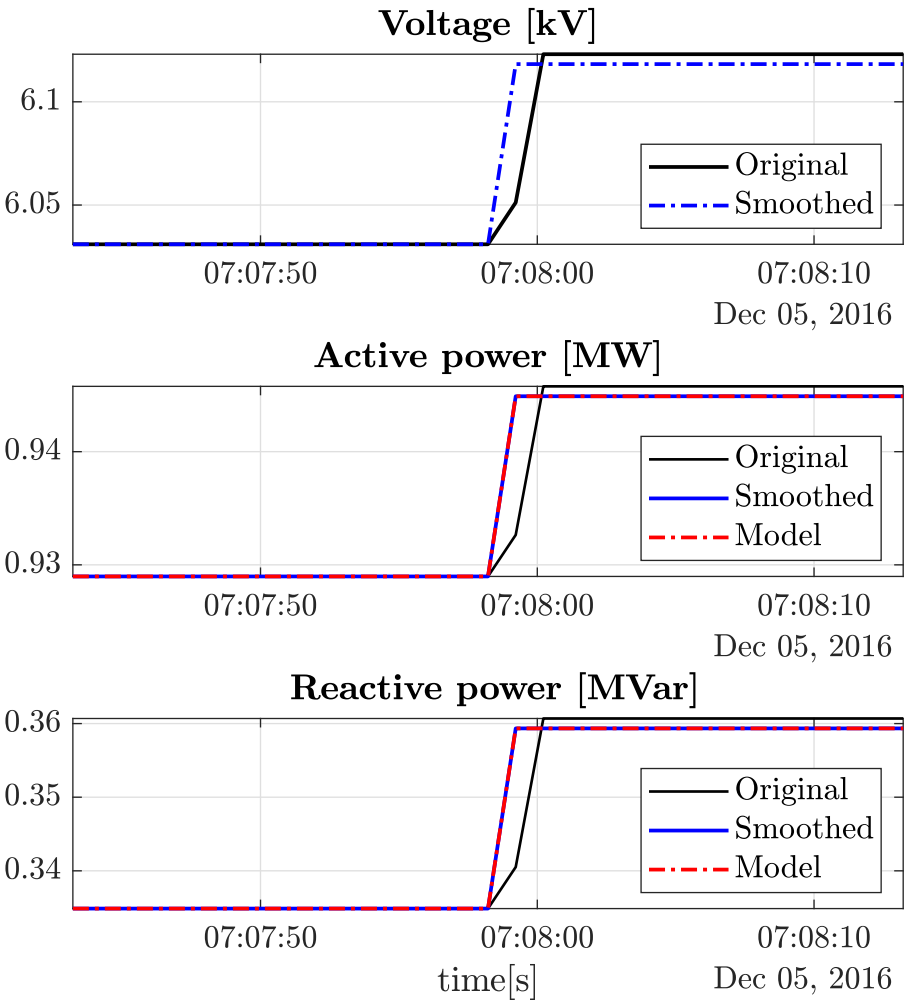

Figure 4.9: Results of measurement based approach applying GA algorithm. The black signal corresponds to the actual or original signal obtained from the field measurements. The signal in blue represents the mean of the original signal before and after the event. The red signal corresponds to the fitted ZIP load model with the obtained parameters of December in table 4.15.

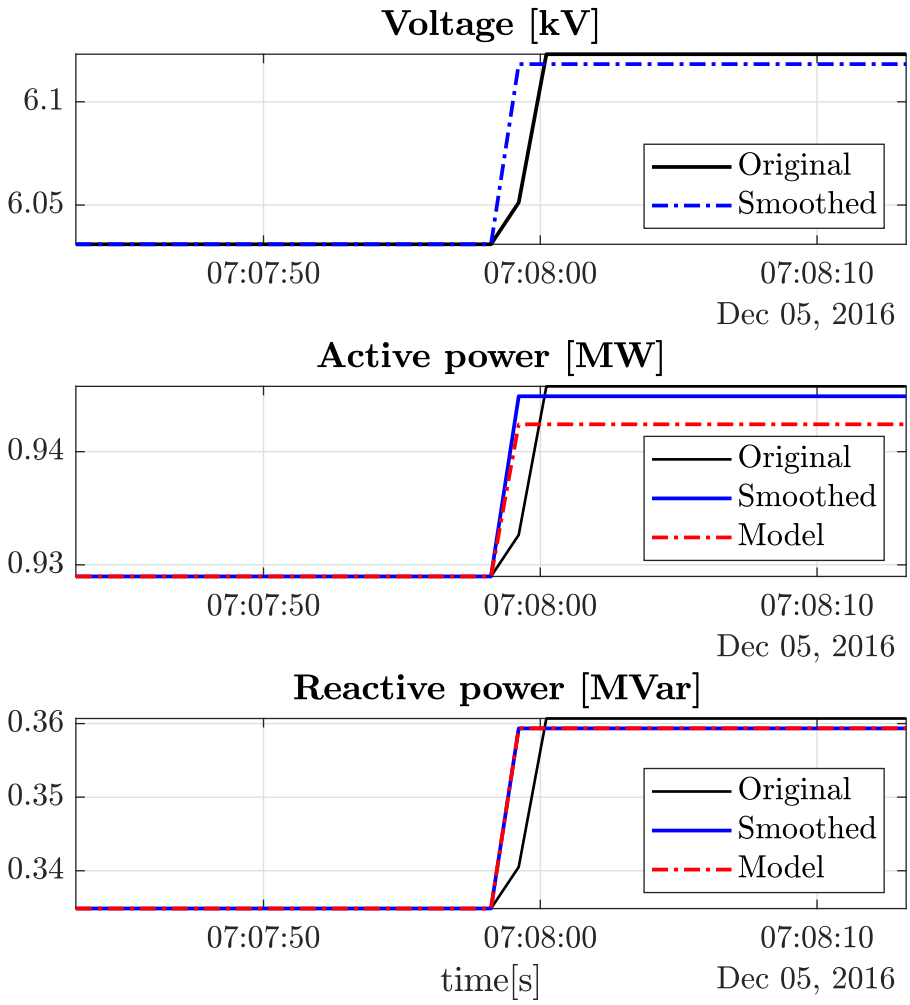

Figure 4.10: Results of measurement based approach applying PSO algorithm. The black signal corresponds to the actual or original signal obtained from the field measurements. The signal in blue represents the mean of the original signal before and after the event. The red signal corresponds to the fitted ZIP load model with the obtained parameters of December in table 4.15.

Table 4.16: The mean absolute percentage error for active and reactive power.

	GA	**PSO**
Dec		
P	0.0095%	1.4581%
Q	0.0001%	0.0001%
Jan		
P	0.1597%	0.1998%
Q	0.1445%	6.0215%
Feb		
P	0.0023%	0.0192%
Q	0.2556%	0.9010%

After checking the instants of the events that occurred in December and January, it was found that both the events happened in working days during the day, thus, the following range can be considered to choose values for the coefficients in winter working days as shown in table 4.17.

Table 4.17: Range of obtained load model coefficients for working days during the day time in Winter.

$\mathbf{Z_p}$	$\mathbf{I_p}$	$\mathbf{P_p}$
(0 - 0.0165)	(0 - 0.0902)	(0.8933 - 1)
$\mathbf{Z_q}$	$\mathbf{I_q}$	$\mathbf{P_q}$
(-0.0274 - 1.5499)	(1.6684 - 1.7509)	(-2.3008 - -0.6410)

Spring

The same procedure was followed for the data that relate to the spring months using the same two algorithms, and table 4.18 represents the obtained coefficients after conducting the two algorithms.

The differences in values of the obtained sets is related to the time at which the event has occurred. For instance, the detected events in April and May took place during the day time whereas for the event that took place in March, it was during the night time. Therefore, the coefficients are taking different values as the load can vary between the different time intervals.

Table 4.18: ZIP load model coefficients obtained using GA and PSO algorithms for Spring.

	Algorithm	$\mathbf{Z_p}$	$\mathbf{I_p}$	$\mathbf{P_p}$	$\mathbf{Z_q}$	$\mathbf{I_q}$	$\mathbf{P_q}$
Mar							
	GA	0.0061	0.0682	0.9257	1.7145	0.5255	-1.2400
	PSO	0	0.1140	0.8859	5.0000	0.9692	-5.0000
Apr							
	GA	0.9821	0.0189	0	3.7810	-2.0577	-0.7233
	PSO	1	0	0	4.9678	1	-5
May							
	GA	0.5627	0.3549	0.0824	2.0328	1.1471	-2.1799
	PSO	0.9228	0.0731	0	5	0.9475	-5

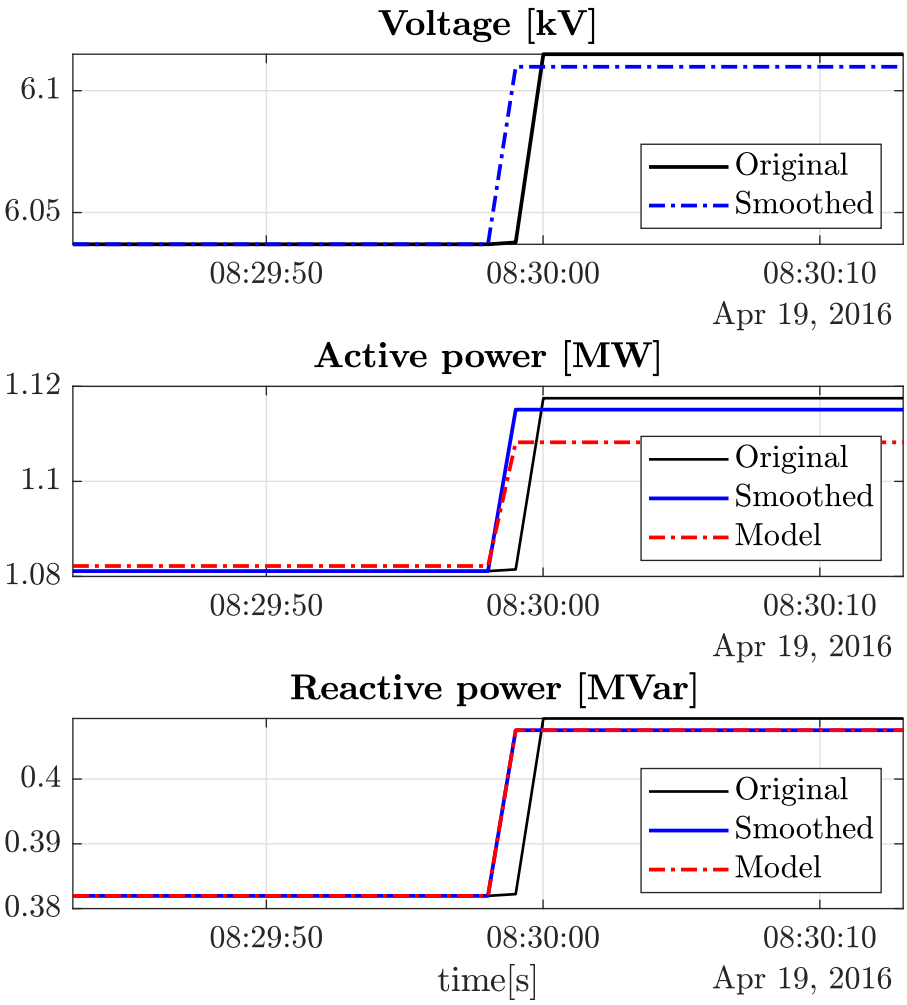

Figure 4.11: Results of measurement based approach applying GA algorithm. The black signal corresponds to the actual or original signal obtained from the field measurements. The signal in blue represents the mean of the original signal before and after the event. The red signal corresponds to the fitted ZIP load model with the obtained parameters of April in table 4.18.

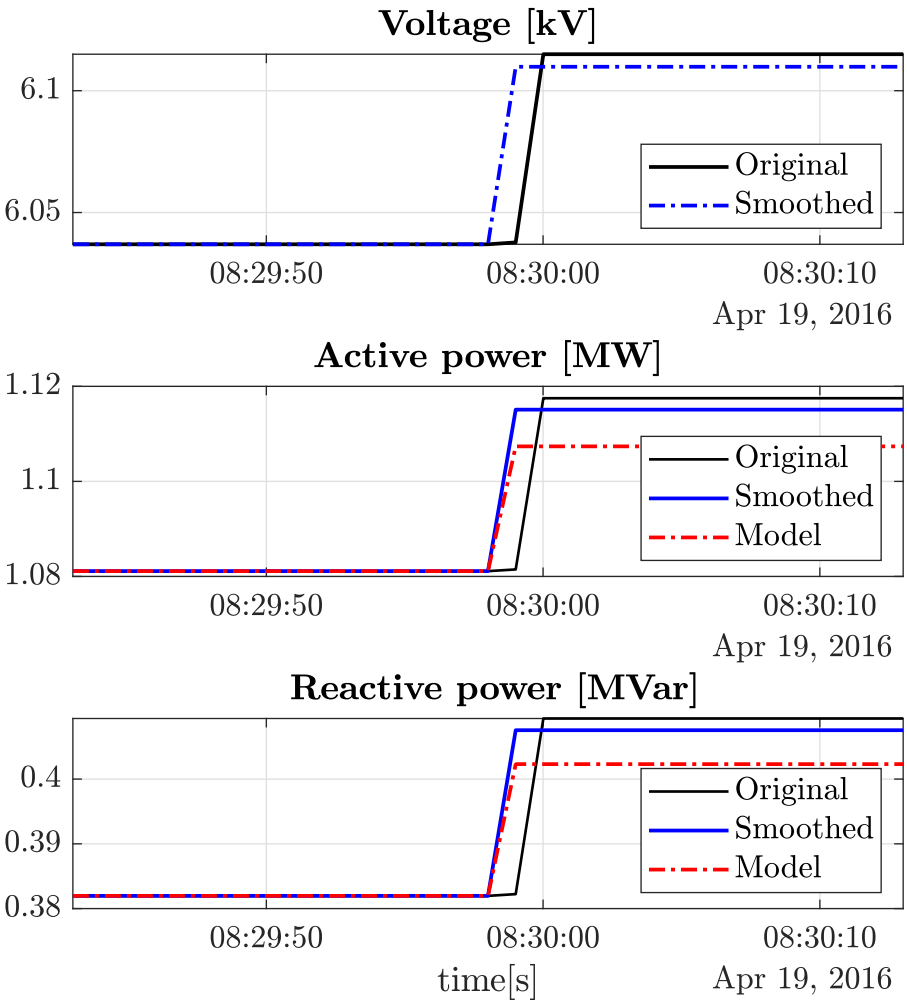

Figure 4.12: Results of measurement based approach applying PSO algorithm. The black signal corresponds to the actual or original signal obtained from the field measurements. The signal in blue represents the mean of the original signal before and after the event. The red signal corresponds to the fitted ZIP load model with the obtained parameters of April in table 4.18.

The corresponding mean absolute error after applying the GA and PSO algorithms in March, April May is given in the table 4.19 below.

Table 4.19: The mean absolute percentage error for active and reactive power.

	GA	**PSO**
Mar		
P	0.0041 %	0.0350%
Q	0.2027%	0.2047%
Apr		
P	0.5189 %	0.5005%
Q	0.4276%	1.0027%
May		
P	0.0115 %	0.4405%
Q	0.0406%	0.2065%

As the events in April and May have accrued in working days during the day time, the following table 4.20 represents the range that the TSO can use to set the parameters values for working days.

Table 4.20: Range of obtained load model coefficients for working days during the day time in Spring.

$\mathbf{Z_p}$	$\mathbf{I_p}$	$\mathbf{P_p}$
(0.5627 - 0.9821)	(0.0189 - 0.3549)	(0 - 0.0824)
$\mathbf{Z_q}$	$\mathbf{I_q}$	$\mathbf{P_q}$
(2.0328 - 3.7810)	(-2.0577 - 1.1471)	(-2.1799 - -0.7233)

Summer

Similar to what has been done so far in previous sections, the data obtained for Summer has been studied and the following results are the study outputs. Table 4.21, shows the results of obtained coefficients after applying the curve-fitting techniques selected.

Table 4.21: ZIP load model coefficients obtained using GA and PSO algorithms for Summer.

	Algorithm	$\mathbf{Z_p}$	$\mathbf{I_p}$	$\mathbf{P_p}$	$\mathbf{Z_q}$	$\mathbf{I_q}$	$\mathbf{P_q}$
Jun							
	GA	0.2318	0.2953	0.4729	2.3892	-0.1406	-1.2487
	PSO	0	1	0	3.9949	0.9652	-3.9871
Jul							
	GA	0.0337	0.0230	0.9433	1.4979	-0.3334	-0.1645
	PSO	0	0.1565	0.8431	3.9646	-0.0442	-2.9531
Aug							
	GA	0.1721	0.5819	0.2459	0.7680	3.0855	-2.8535
	PSO	0	1	0	4.9968	0.9739	-5.0000

Figures 4.14 and 4.13 show the original signal and the resulted model signal.

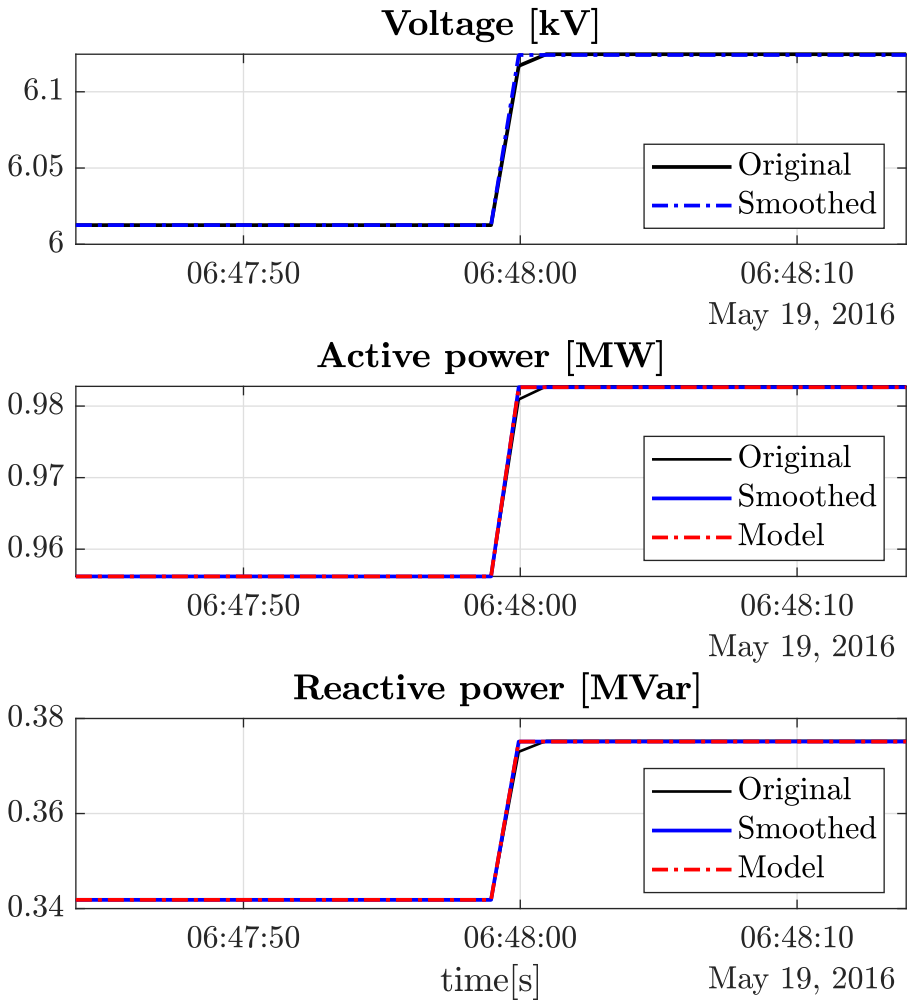

Figure 4.13: Results of measurement based approach applying GA algorithm. The black signal corresponds to the actual or original signal obtained from the field measurements. The signal in blue represents the mean of the original signal before and after the event. The red signal corresponds to the fitted ZIP load model with the obtained parameters of May in table 4.21.

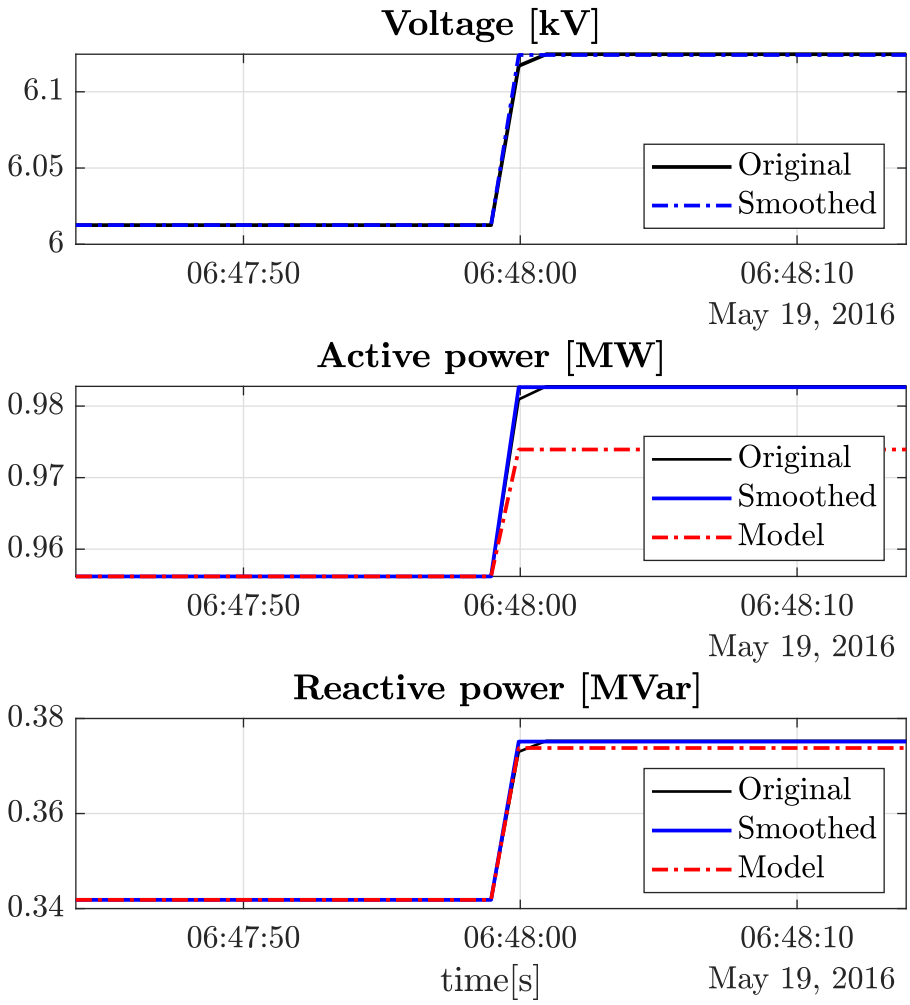

Figure 4.14: Results of measurement based approach applying PSO algorithm. The black signal corresponds to the actual or original signal obtained from the field measurements. The signal in blue represents the mean of the original signal before and after the event. The red signal corresponds to the fitted ZIP load model with the obtained parameters of May in table 4.21.

Table 4.22 shows the mean absolute error after applying GA and PSO algorithms. Table 4.23 further gives a range of values from which the TSO can choose coefficients values for the summer working days.

Table 4.22: The mean absolute percentage error for active and reactive power.

	GA	**PSO**
Jun		
P	0.0017%	0.1484%
Q	0.0102%	0.4791%
Jul		
P	0.0065%	0.0558%
Q	0.1914%	1.3640%
Aug		
P	0.0143%	0.0330%
Q	0.0715%	0.2031%

Table 4.23: Range of obtained load model coefficients for working days during the day time in Summer.

$\mathbf{Z_p}$	$\mathbf{I_p}$	$\mathbf{P_p}$
(0.0337 - 0.1721)	(0.0230 - 0.5819)	(0.2459 - 0.9433)
$\mathbf{Z_q}$	$\mathbf{I_q}$	$\mathbf{P_q}$
(0.7680 - 1.4979)	(-0.3334 - 3.0855)	(-0.1645 - -2.8535)

Autumn

Finally, the data related to September, October and November months have been analyzed and the voltage events in these months were detected. Table 4.24 shows the different sets of coefficients obtained, and table 4.25 gives the mean absolute error after applying the curve fitting algorithms.

Table 4.24: ZIP load model coefficients obtained using GA and PSO algorithms for Spring.

	Algorithm	$\mathbf{Z_p}$	$\mathbf{I_p}$	$\mathbf{P_p}$	$\mathbf{Z_q}$	$\mathbf{I_q}$	$\mathbf{P_q}$
Sep							
	GA	0.0001	0.0253	0.9746	1.3941	0.7182	-1.1123
	PSO	0.0187	0	0.9812	3.5385	2.0304	-4.5921
Oct							
	GA	0.4766	0.1938	0.3296	2.8503	0.2576	-2.1079
	PSO	0.2754	0.7237	0	3.9278	2.0433	-5.0000
Nov							
	GA	0	0	1	-0.0060	0.3868	0.6192
	PSO	0	0	1	-0.0457	3.0845	-5.0000

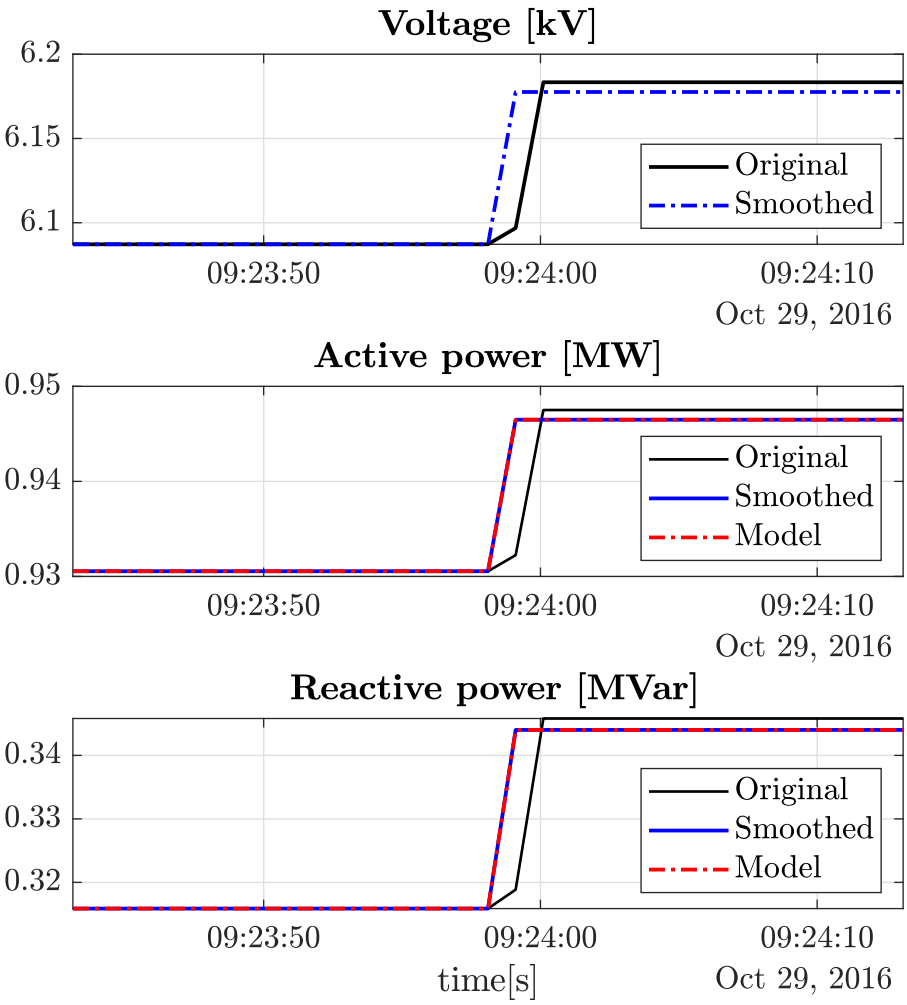

Figure 4.15: Results of measurement based approach applying GA algorithm. The black signal corresponds to the actual or original signal obtained from the field measurements. The signal in blue represents the mean of the original signal before and after the event. The red signal corresponds to the fitted ZIP load model with the obtained parameters of October in table 4.24.

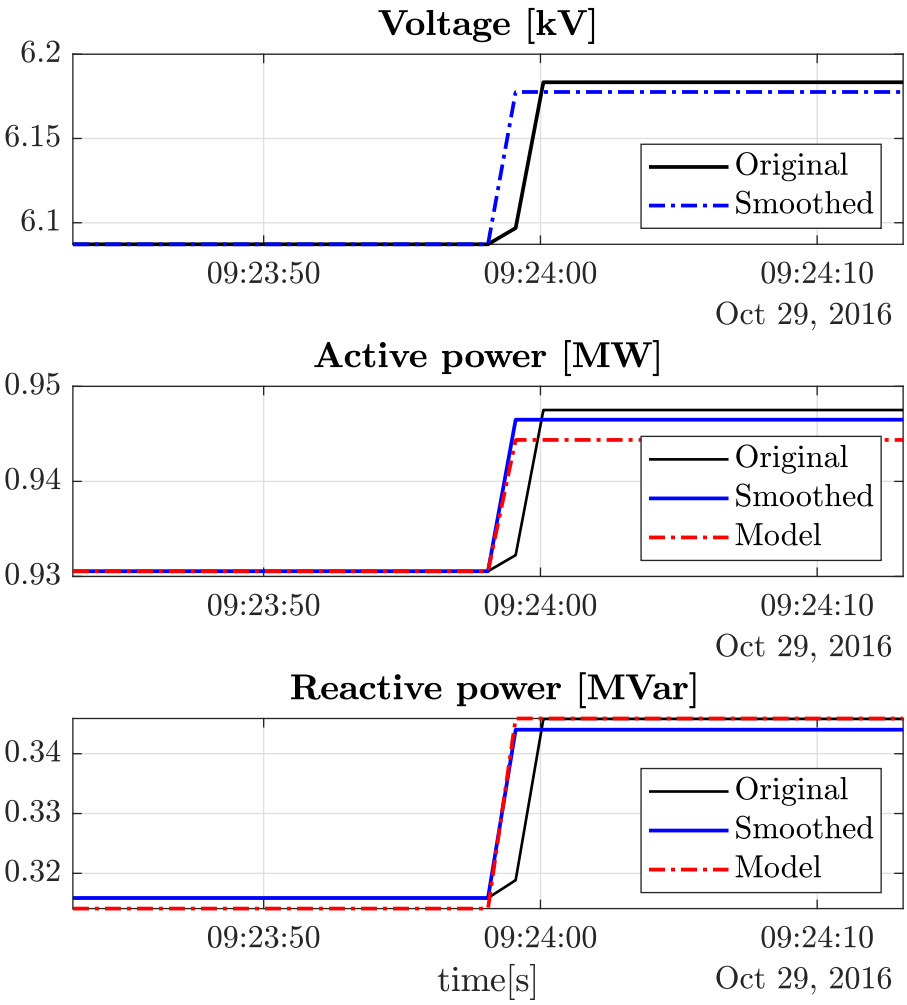

Figure 4.16: Results of measurement based approach applying PSO algorithm. The black signal corresponds to the actual or original signal obtained from the field measurements. The signal in blue represents the mean of the original signal before and after the event. The red signal corresponds to the fitted ZIP load model with the obtained parameters of October in table 4.24.

Table 4.25: The mean absolute percentage error for active and reactive power.

	GA	**PSO**
Sep		
P	0.0014%	0.8547%
Q	0.0104%	0.3648%
Oct		
P	0.0988%	0.1947%
Q	0.5139%	0.5752%
Nov		
P	0.5343%	0.5864%
Q	6.0214%	6.0214%

As the events in September and October have occurred in weekends, the range in table 4.26 can be considered when setting the coefficients for weekends in Autumn.

Table 4.26: Range of obtained load model coefficients for weekends day time in Autumn.

$\mathbf{Z_p}$	$\mathbf{I_p}$	$\mathbf{P_p}$
(0.0001 - 0.4766)	(0.0253 - 0.1938)	(0.3296 - 0.9746)
$\mathbf{Z_q}$	$\mathbf{I_q}$	$\mathbf{P_q}$
(1.3941 - 2.8503)	(0.2576 - 0.7182)	(-2.1079 - -1.1123)

4.3 Verification of obtained coefficients

In this section, the parameters obtained will be tested using a simplified system built in PSS/E. The main goal of this test is to observe the changes in voltage at the load bus when different sets of coefficients are used. In addition, the corresponding load behaviour represented in the active and reactive power responses will be analysed.

4.3.1 Test model

In the test system represented in Figure 4.17, the change in voltage at bus 11 has occurred after causing a fault in the system. The fault has been chosen to be a line trip between buses 6 and 7. Conversion of the load was conducted by applying several combinations of the ZIP coefficients. These combinations applied to the load connected to bus 11 include constant impedance, constant current, constant power as well as sets of parameters obtained after applying the curve-fitting algorithms on the real data as explained in the previous sections.

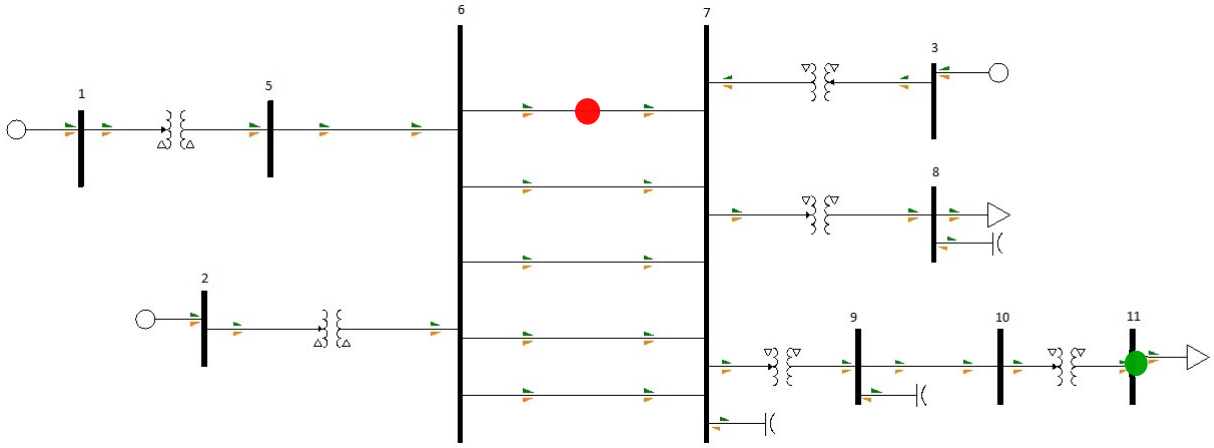

Figure 4.17: Test model in PSS/E, where the red circle represents the fault location and the green circle is the load bus at which the load response is studied.

4.3.2 Constant impedance load

The first case to start with is the constant impedance load. Thus, the load at bus 11 was considered as a constant impedance load by changing the parameters Z_p and Z_q in PSS/E to take the value of one and setting the remaining parameters I_p, P_p, I_q and P_q to zero. After tripping the line between buses 6 and 7 the voltage behaviour at bus 11 and both the active and reactive responses of the load are given in the figure 4.18.

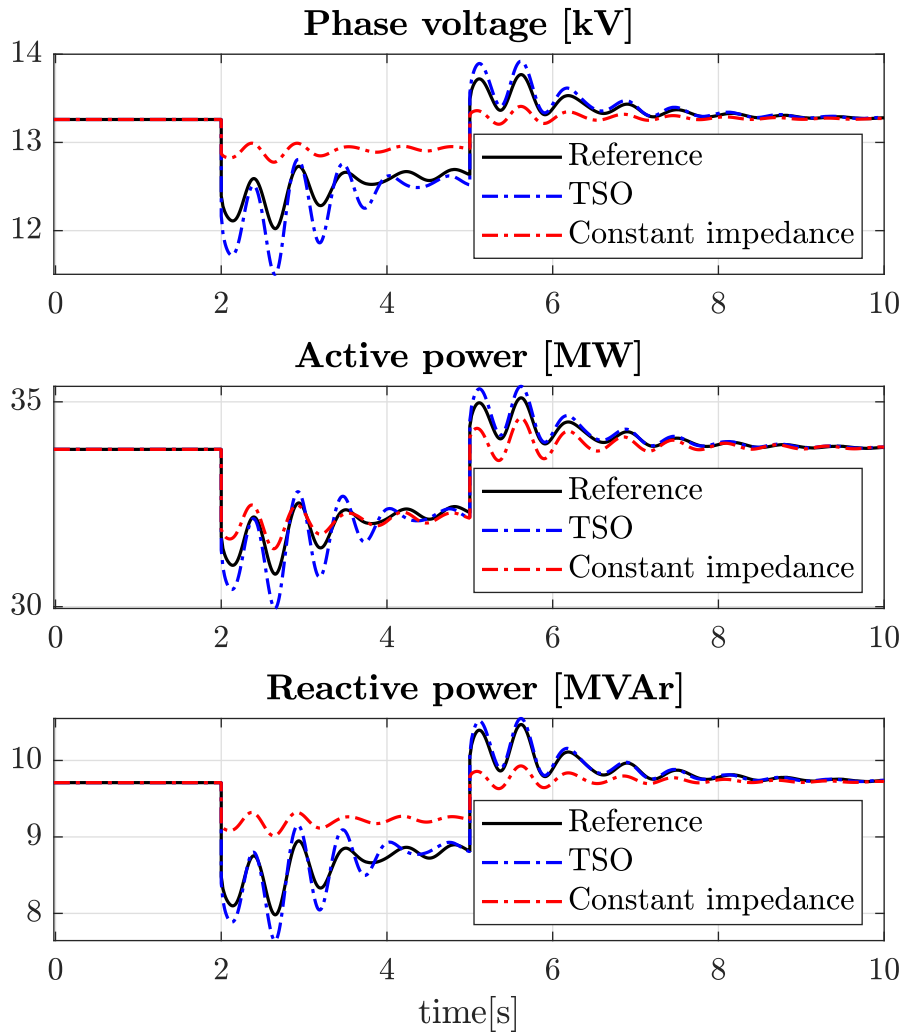

Figure 4.18: Voltage and load response at load bus 11 before and after the event for different ZIP load coefficients.

In Figure 4.18 the reference signal corresponds to the voltage and the load response when the load was modelled by the ZIP coefficients obtained in the case study of s Sections 4.1 and 4.2. The blue and the red signals represent the voltage and the load responses with the TSO parameters and ZIP coefficients of the constant impedance, respectively. In the test system as shown in Figure 4.17, the fault represented by the line trip between buses 6 and 7 has been applied at the two second after the steady state period. The fault has been cleared by reconnecting the line again after 3 seconds which represents the fault duration. The post fault period starts at the fifth second, and the simulation time was set to be 10 seconds including the fault duration.

According to the results presented in table 4.27, the active and reactive power responses during the fault and after clearing it, have more reliable performance than the responses acquired after using the TSO's parameters.

Table 4.27: The mean absolute percentage error for active and reactive power.

	P error	**Q error**
TSO		
	2.6155%	1.4950%
$Z_p, Z_q = 1$		
	0.4673%	1.1174%

4.3.3 Constant current load

In this case, constant current load is implemented by having I_p and I_q equal to one and the rest of the parameters equal to zero for the load at bus 11 in 4.17. Similarly, the same fault applied in the first case has been applied again, and the results obtained are compared with the TSO's parameters and those found after conducting the study on the real measurements in sections 4.1 and 4.2. It can be observed in figure 4.19, that the TSO coefficients result in the same behaviour of voltage and load response as in the first case. This is due to the fact that TSO uses same set of coefficients to model the load.

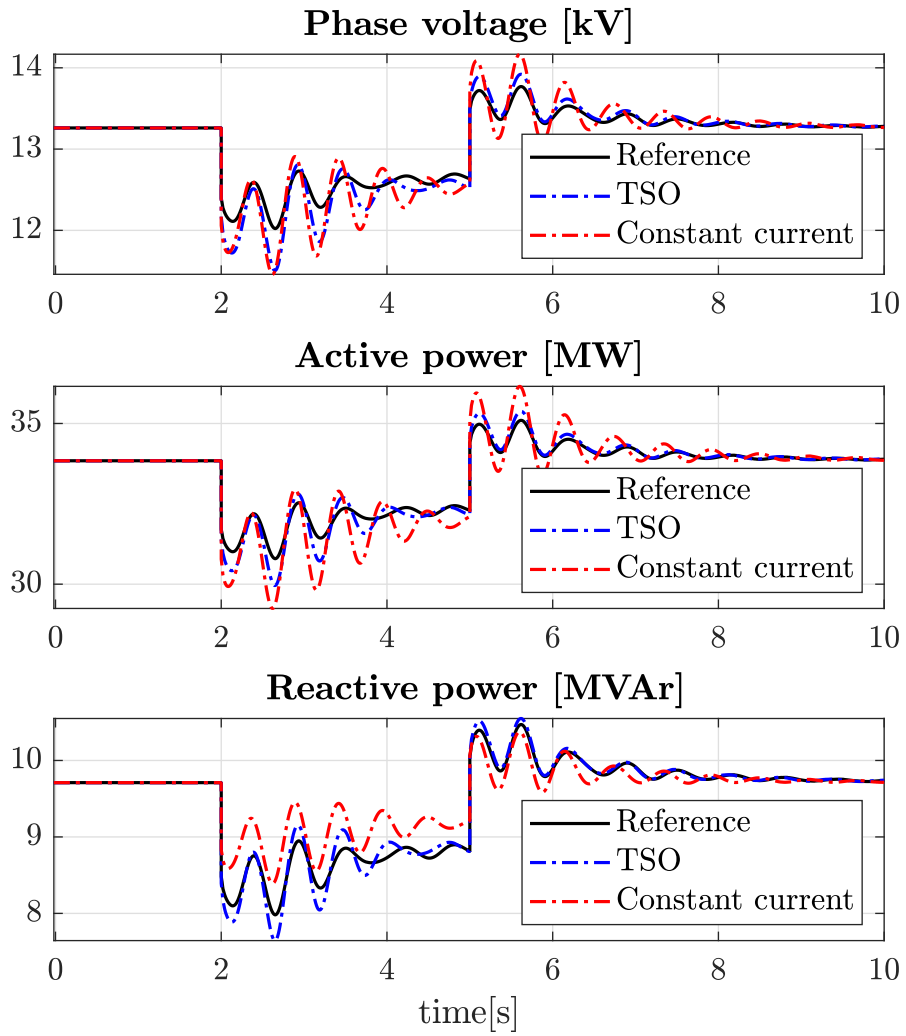

Figure 4.19: Voltage and load response at load bus 11 before and after the event for different ZIP load coefficients.

Results obtained after calculating the mean absolute error are shown in table 4.28. It can be noticed that the constant current load is achieve better performance than the TSO's parameters, as it has less error and is closer to the reference signal.

Table 4.28: The mean absolute percentage error for active and reactive power.

	P error	**Q error**
TSO		
	2.6155%	1.4950%
$I_p, I_q = 1$		
	1.1992%	0.8652%

4.3.4 Constant power load

The last case of load, namely the constant power load, is also applied for the load at the bus 11 in 4.17. The active power parameters of the load P_p and P_q are given the value one while the impedance and the current parameters are set to zero. The fault as defined before, has been applied in order to check both the voltage and load behaviour at bus 11. This behavior will be compared again with the TSO's parameters and the parameters obtained from the study conducted in 4.1 and 4.2. It can be clearly observed in figure 4.20 (for the case of constant power load) that the voltage response before, during and after clearing the fault shows that it has many high frequency oscillations that resulted because of the numerical errors that occurred upon applying the constant power load. Therefore, the voltage signal has been filtered as shown in the second subplot in 4.20 in order to obtain the expected curve of voltage.

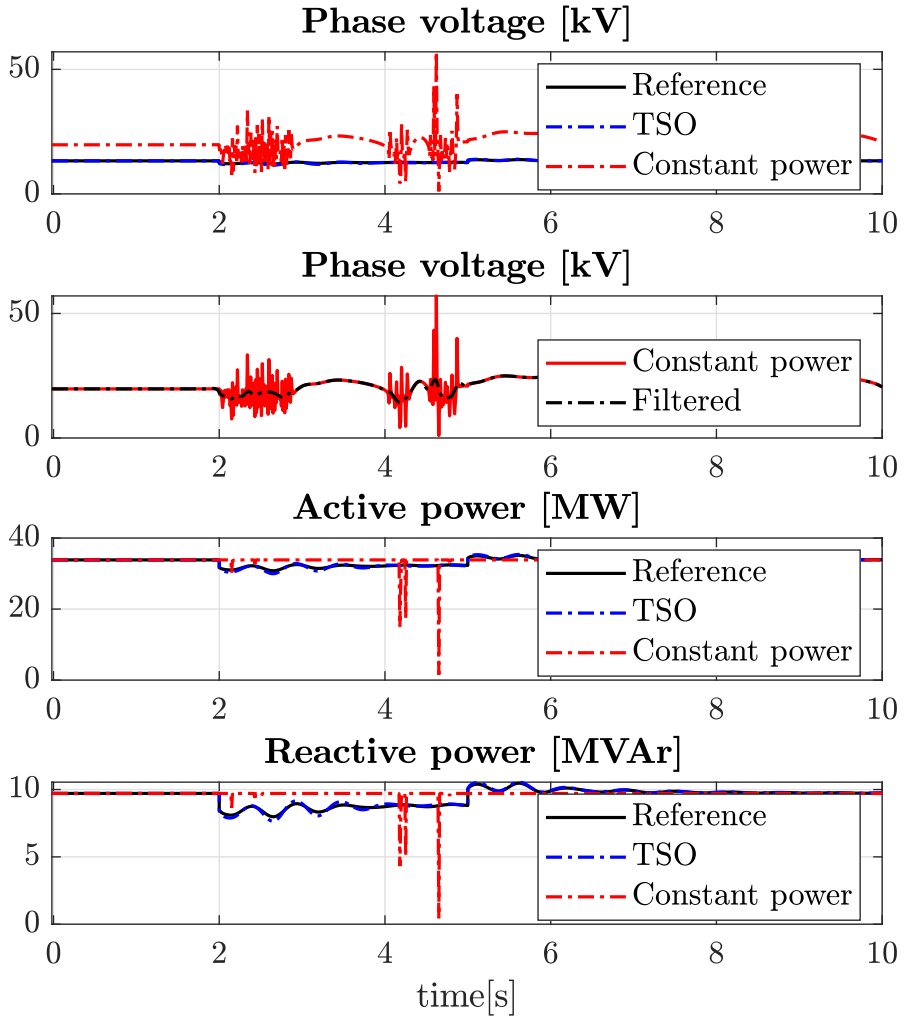

Figure 4.20: Voltage and load response at load bus 11 before and after the event for different ZIP load coefficients.

Table 4.29 shows the mean absolute error in active and reactive power between two different cases of load model: constant power load and one Nordic TSO set of coefficients, and the reference signal corresponds to the study parameters.

Table 4.29: The mean absolute percentage error for active and reactive power.

	P error	**Q error**
TSO		
	2.6155%	1.4950%
$P_p, P_q = 1$		
	2.4464%	1.7941%

4.3.5 Nordic TSO's load parameters

Figure 4.22 presents the voltage response and the load responses in active and reactive power for different sets of coefficients. These coefficients are related to several TSOs in the Nordic countries and used by these TSOs for the load modelling purposes.

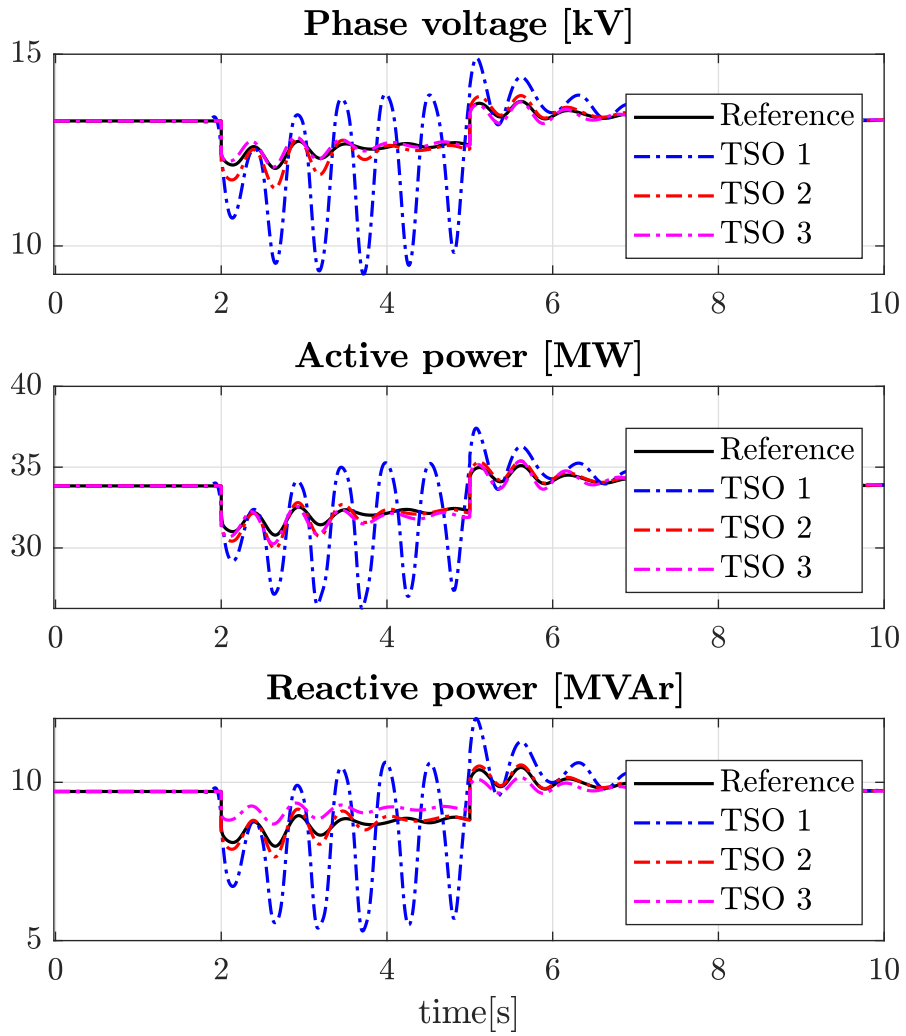

Figure 4.21: Voltage and load response at load bus 11 before and after the event using different ZIP load coefficients of Nordic TSOs.

Table 4.30 shows the mean absolute error between the reference signal and the signals related to the different TSOs. The reference signal represents either the active or reactive power response after applying the load model with the coefficients obtained from the study discussed in sections 4.1 and 4.2. The signals TSO1, TSO2 and TSO3 are the active and reactive power responses after applying the coefficients of different Nordic TSOs, and calculating the error between each of them and the reference. It can be observed that the signals resulting in TSO2's parameters are the closest ones to the reference signal. TSO1's load parameters relatively significant deviation comparing to the other responses. The reason behind this can be due to the conservative choice of constant power load which can mismatch the actual load composition.

Table 4.30: The mean absolute percentage error for active and reactive power.

	P error	Q error
TSO 1		
	2.616%	1.495%
TSO 2		
	0.646%	0.391%
TSO 3		
	0.769%	0.952%

4.3.6 Nordic32 test model

After applying the obtained parameters in the previous simplified test system, the Nordic 32 system was selected to test these parameters and observe the load responses in active and reactive power. Nordic 32 test system is widely used in the TSOs and academic studies since the dynamic properties available in this system are quite similar to the Swedish and Nordic power systems.

4.3.6.1 Nordic TSO's load parameters for Nordic32 system

Figure 4.22, shows the voltage response and the load responses in active and reactive power for different load parameters in the Nordic32 test model. These coefficients are related to several TSOs in the Nordic countries and used by them for the load modelling purposes.

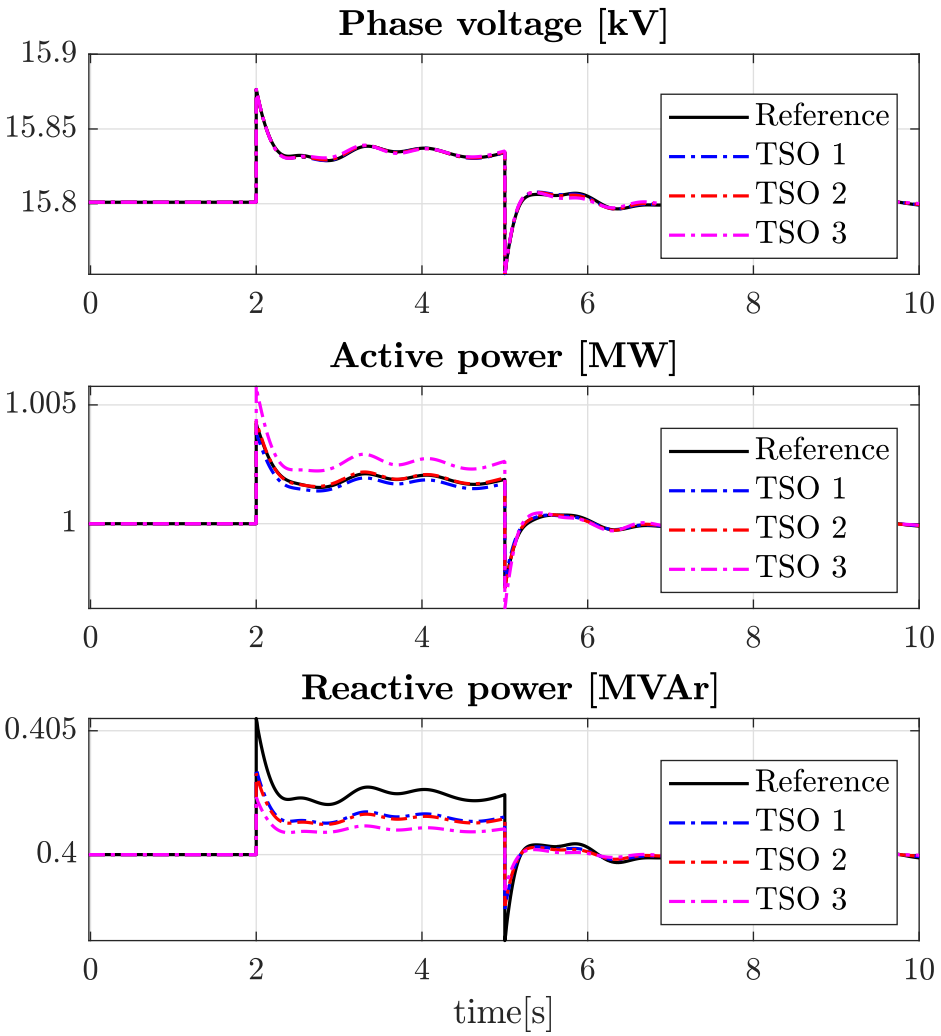

Figure 4.22: Voltage and load response for different coefficients used by Nordic TSOs.

Table 4.31 shows that the mean absolute error between the reference signal and the signals corresponding to the different TSOs are very small. In other words, the applied load parameters of different Nordic TSOs are close to the realistic load parameters obtained from the case studies.

Table 4.31: The mean absolute percentage error for active and reactive power.

	P error	**Q error**
TSO 1		
	0.007%	0.032%
TSO 2		
	0.002%	0.035%
TSO 3		
	0.024%	0.051%

5
Discussion

After selecting the measurement based approach, and applying two different curve-fitting techniques, the results obtained are summarized in table 5.1. This table contains one set of parameters obtained from the case study explained in section 4 and different sets of coefficients used by different Nordic TSOs.

Table 5.1: ZIP parameters obtained from the study and the current choices of parameters of Nordic TSOs.

ZIP parameters	$\mathbf{Z_p}$	$\mathbf{I_p}$	$\mathbf{P_p}$	$\mathbf{Z_q}$	$\mathbf{I_q}$	$\mathbf{P_q}$
Measurement-based	0.19	0.48	0.33	0.99	0.87	-0.86
TSO 1	0.40	0	0.60	0.90	0	0.10
TSO 2	0.25	0.40	0.35	0.70	0.30	0
TSO 3	0.40	0.40	0.20	0.40	0.40	0.20

As can be observed from table 5.1, the parameters chosen by the Nordic TSOs took the values between zero and one. On the other hand, for the parameters obtained after conducting this study, only the active power coefficients were constrained to be in the interval $[0, 1]$, whereas for reactive power coefficients this constraint was not considered. Therefore, it can be noticed that P_q coefficient is taking a negative value. However, all the forementioned sets of coefficients are constrained to the same condition of having the sum of all coefficients to be one.

Generally, both GA and PSO algorithms used in this study result in different results of load parameters that can yield a good curve-fitting with active and reactive power of the real system. As the GA algorithm gave results with less error, it was chosen later to be the algorithm whose parameters are the reference.

In order to compare the performance of different load parameters, a simplified test model shown in figure 4.17 was built, and a line trip fault was introduced to cause a voltage disturbance and observe the behaviour of the load. Due to the lack of knowledge about the load composition, the general conventional load types of constant impedance, constant current and constant power were used to model the load. This comparison yields a possibility to compare the load responses in each conventional type with the TSOs models and the model of the study.

For the case of constant power load, voltage and load responses in active and reactive power were not as expected. The reason behind that could be numerical issues in

PSS/E software. Therefore, the voltage signal was filtered in order to obtain the expected voltage. However, all the sets of coefficients that are currently employed by the Nordic TSOs lead to close results, and this is revealed from the error calculated in table 4.30.

When using the Nordic 32 test model, similar results were obtained after applying different sets of coefficients used by the Nordic TSOs. However, the mean absolute error between the Nordic TSOs coefficients and the reference set obtained from this study was calculated in order to compare how close these coefficients are to the reference. As the results are not so significant, that leads to the fact that the Nordic TSOs coefficients are sufficiently close to the reference load parameters.

5.1 Sustainability and ethical aspects

Having a reliable load model that can be applied in the test model systems have big importance in power systems operations. As loads represent an essential part of any power system, an accurate load model is required to understand the behaviour of the load in the real system. Subsequently, transmission system operators will be able to conduct future studies on the system in terms of future plans that ensure practical, environmental and economical efficiency in the system. Moreover, these test models mimic the real systems, thus, the system operator will have the possibility to simulate the scenarios that may occur in the system and take the right decisions if any similar event takes place in the real network.

Furthermore, these test models can be used for educational purposes in order to help students understand the real power system operations and contribute with their new ideas and thoughts to support the sustainability of the electric power systems. Also, these models represent the base on which lots of research and development work can be done.

The ethical aspects were strictly followed in this work. This commitment was represented in keeping the secrecy of the data received from the Nordic DSOs. Also, an ideal usage of these data was determined as they were the main source from which the results were obtained.

The objective from this work is centered around improving the existing ZIP load model parameters used by the TSOs. It was important in this study to verify the performance and correctness of the obtained parameters using practically used test models.

6
Conclusion

Load modeling is one of the most important tasks in power system operations. Acquiring a reliable load model is always faced by several challenging issues including the variety and complexity in loads characteristics, differences in the load composition between the evaluation points as well as the changing behaviour of the load among the different seasons of the year.

6.1 Measurement-based approach

This approach relies mainly on the data obtained from the real power system and more data supplied by the local DSOs helps to achieve more accurate parameters which in turn result in more reliable models for the load. Moreover, measurement-based approach allows to apply different algorithms for the curve-fitting purposes. Therefore, this approach ensures high level of flexibility as each curve-fitting technique leads to different sets of coefficients that can give acceptable results. The TSO will eventually have the decision to choose the suitable set of parameters corresponding to the different seasons that achieve the most realistic results based on its criteria.

On the other hand, it was observed that the measurement-based approach did not give accurate results when the voltage step was not significant enough (the deviation in voltage is less than 1.5%) or when the reactive power parameters were constrained to take the values between [0,1].

6.2 Future work

Last but not least, different points of interest for further study are mentioned in this section such as:

- Frequency dependency of the load.
- Automazation of voltage events detecting process in order to achieve the purposes fast and more efficiently.
- Introducing different events in the system to verify the obtained load model after studying the load behaviour resulting of these events.
- In case more information are supplied about the load class and its composition, 'Component-based approach' can be used in parallel with 'Measurement-based approach' to obtain more accurate and reliable results.

Bibliography

[1] K. Walve, "Modeling of power system components at severe disturbances," in *International Conference on Large High Voltage Electric Systems (August 1986)*, 1986.

[2] W. Price, C. Taylor, and G. Rogers, "Standard load models for power flow and dynamic performance simulation," *IEEE Transactions on power systems*, vol. 10, no. CONF-940702-, 1995.

[3] W. Price, H. Chiang, H. Clark, C. Concordia, D. Lee, J. Hsu, S. Ihara, C. King, C. Lin, Y. Mansour, *et al.*, "Load representation for dynamic performance analysis," *IEEE Transactions on Power Systems (Institute of Electrical and Electronics Engineers);(United States)*, vol. 8, no. 2, 1993.

[4] S. Ab, "Understanding and modelling of load in the power system," p. 2017, 2017.

[5] "2016 - CIGRE - Load modelling Part 1 - Method development - published - C4-104.pdf."

[6] "STRI - R16-1239 - SP2 - Method verification ."

[7] H.-D. Chiang, J.-C. Wang, C.-T. Huang, Y.-T. Chen, and C.-H. Huang, "Development of a dynamic zip-motor load model from on-line field measurements," *International Journal of Electrical Power & Energy Systems*, vol. 19, no. 7, pp. 459–468, 1997.

[8] H. Saadat, *Power System Analysis McGraw-Hill Series in Electrical Computer Engineering*. 1999.

[9] D. N. Kosterev, C. W. Taylor, and W. A. Mittelstadt, "Model validation for the august 10, 1996 wscc system outage," *IEEE Transactions on Power Systems*, vol. 14, pp. 967–979, Aug 1999.

[10] "C 4 -104 CIGRE 2016 Development of improved aggregated load models for power system network planning in the Nordic power system Part 1 : Method development Emil.Hillberg@stri.se," 2016.

[11] "DUBLIN 2017 Understanding and modelling of load in the power system STRI AB , 2 KTH Adriel.Perez@stri.se," 2017.

[12] D. Karlsson and D. J. Hill, "Modelling and identification of nonlinear dynamic loads in power systems," *IEEE Transactions on Power Systems*, vol. 9, no. 1, pp. 157–166, 1994.

[13] J. V. Milanovic, K. Yamashita, S. M. Villanueva, S. Ž. Djokic, and L. M. Korunović, "International industry practice on power system load modeling," *IEEE Transactions on Power Systems*, vol. 28, no. 3, pp. 3038–3046, 2013.

[14] A. Oonsivilai and M. El-Hawary, "Power system dynamic load modeling using adaptive-network-based fuzzy inference system," in *Electrical and Computer*

Engineering, 1999 IEEE Canadian Conference on, vol. 3, pp. 1217–1222, IEEE, 1999.

[15] H. Zeineldin and J. L. Kirtley Jr, "Performance of the ovp/uvp and ofp/ufp method with voltage and frequency dependent loads," *IEEE Transactions on Power Delivery*, vol. 24, no. 2, pp. 772–778, 2009.

[16] N. Mohan, T. M. Undeland, and W. P. Robbins, "Power electronics: converters, applications, and design," 1995.

[17] K. McKenna and A. Keane, "Electrical and thermal characteristics of household appliances: Voltage dependency, harmonics and thermal rc parameters," tech. rep., 2016.

[18] F. S. Chassin, E. T. Mayhorn, M. A. Elizondo, and S. Lu, "Load modeling and calibration techniques for power system studies," in *2011 North American Power Symposium*, pp. 1–7, IEEE, 2011.

[19] M. E.-N. Jahromi and M. T. Ameli, "Measurement-based modelling of composite load using genetic algorithm," *Electric Power Systems Research*, vol. 158, pp. 82–91, 2018.

[20] H. Renmu, M. Jin, and D. J. Hill, "Composite load modeling via measurement approach," *IEEE Transactions on Power Systems*, vol. 21, no. 2, pp. 663–672, 2006.

[21] E. O. Kontis, T. A. Papadopoulos, A. I. Chrysochos, and G. K. Papagiannis, "Measurement-based dynamic load modeling using the vector fitting technique," *Trans. Power Syst*, 2018.

[22] H. Bai, P. Zhang, and V. Ajjarapu, "A novel parameter identification approach via hybrid learning for aggregate load modeling," *IEEE Transactions on power systems*, vol. 24, no. 3, pp. 1145–1154, 2009.

[23] M. Jin, H. Dong, and R. He, "Measurement-based load modeling: Theory and application," *Science in China Series E: Technological Sciences*, vol. 50, no. 5, pp. 606–617, 2007.

[24] H. You, X. Jianjuan, and G. Xin, *Radar data processing with applications*. John Wiley & Sons, 2016.

[25] H. Motulsky and A. Christopoulos, *Fitting models to biological data using linear and nonlinear regression: a practical guide to curve fitting*. Oxford University Press, 2004.

[26] W. H. Press, *Numerical recipes C diskette V1. 3: format IBM PC, PS/2, and compatibles (DOS)*. Cambridge University Press, 1988.

[27] R. W. Stineman, "A consistently well-behaved method of interpolation," *Creative Computing*, 1980.

[28] J. Chambers, W. Cleveland, B. Kleiner, and P. Tukey, "Graphical methods for data analysis duxbury press," *Massachusetts, USA: Boston*, 1983.

[29] K. Yamashita, S. M. Villanueva, and J. Milanovic, "Initial results of international survey on industrial practice on power system load modelling conducted by cigre wg c4. 605," in *Proc. CIGRE Symp.*, vol. 4, 2011.

[30] D. S. W. Pollard, S. Ranade, *Advanced Load Modeling - Entergy Pilot Study*. 2004.

[31] A. Arabali, M. Ghofrani, M. Etezadi-Amoli, M. S. Fadali, and Y. Baghzouz, "Genetic-algorithm-based optimization approach for energy manage-

ment," *IEEE Transactions on Power Delivery*, vol. 28, no. 1, pp. 162–170, 2013.

[32] K. Deb, A. Pratap, S. Agarwal, and T. Meyarivan, "A fast and elitist multiobjective genetic algorithm: Nsga-ii," *IEEE transactions on evolutionary computation*, vol. 6, no. 2, pp. 182–197, 2002.

[33] R. Eberhart and J. Kennedy, "A new optimizer using particle swarm theory," in *MHS'95. Proceedings of the Sixth International Symposium on Micro Machine and Human Science*, pp. 39–43, Ieee, 1995.

[34] G. A. Barzegkar-Ntovom, O. Ceylan, and T. A. Papadopoulos, "Optimization techniques for parameter estimation of dynamic load models," in *2017 52nd International Universities Power Engineering Conference (UPEC)*, pp. 1–6, IEEE, 2017.

[35] Y. Shi *et al.*, "Particle swarm optimization: developments, applications and resources," in *Proceedings of the 2001 Congress on Evolutionary Computation (IEEE Cat. No. 01TH8546)*, vol. 1, pp. 81–86, IEEE, 2001.

A

Appendix 1

A.1 Winter-based study for evaluation point 3

Table A.1: ZIP load model coefficients obtained using GA for Winter.

	Algorithm	$\mathbf{Z_p}$	$\mathbf{I_p}$	$\mathbf{P_p}$	$\mathbf{Z_q}$	$\mathbf{I_q}$	$\mathbf{P_q}$
Dec							
	GA	0.0040	0.0969	0.8990	2.5003	0.2000	-1.7004
Jan							
	GA	0.0030	0.1173	0.8797	2.5213	0.2013	-1.3200
Feb							
	GA	0.0073	0.0292	0.9635	3.5868	-2.3008	-0.2860

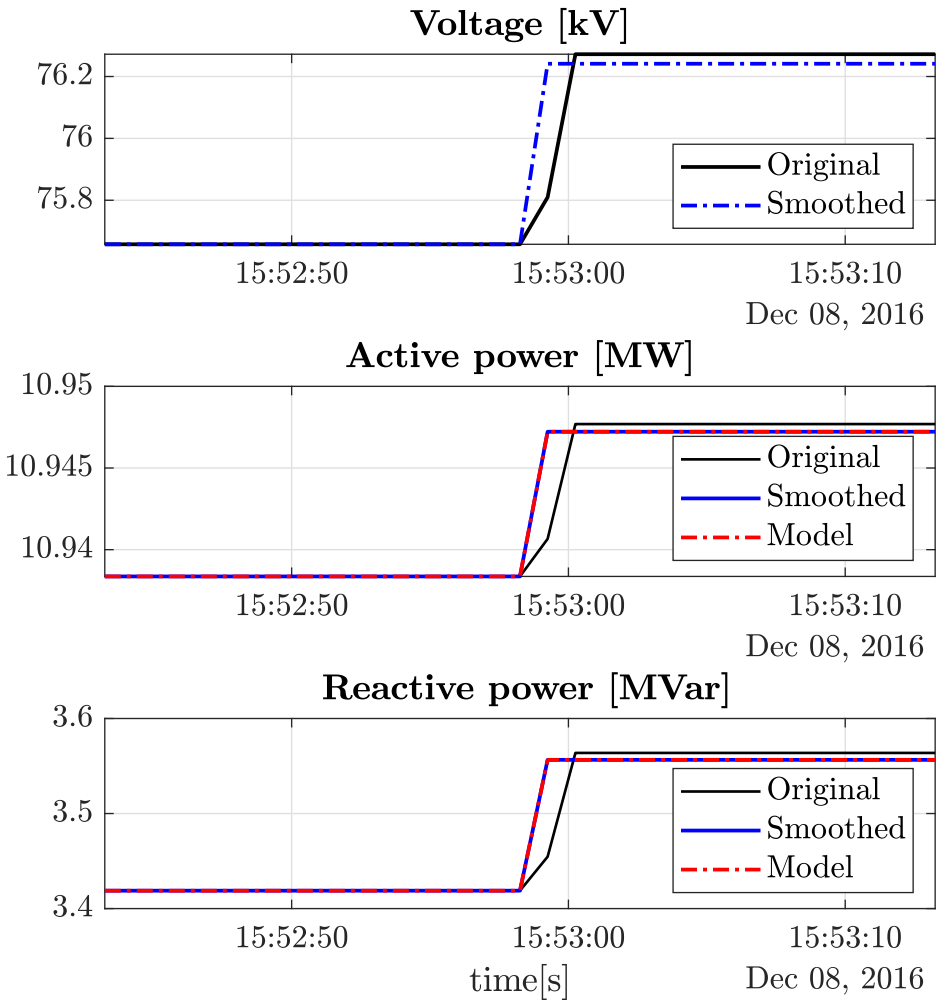

Figure A.1: Results of measurement based approach applying GA algorithm. The black signal corresponds to the actual or original signal obtained from the field measurements. The signal in blue represents the mean of the original signal before and after the event. The red signal corresponds to the fitted ZIP load model with the obtained parameters of December in table A.1.

Table A.2: Range of obtained load model coefficients for working days during the day time in Autumn.

$\mathbf{Z_p}$	$\mathbf{I_p}$	$\mathbf{P_p}$
(0.0030 - 0.0073)	(0.0292 - 0.1173)	(0.8797 - 0.9635)
$\mathbf{Z_q}$	$\mathbf{I_q}$	$\mathbf{P_q}$
(2.5003 - 3.5868)	(-2.3008- 0.2013)	(-1.7004 - -0.2860)

A.2 Spring-based study for evaluation point 3

Table A.3: ZIP load model coefficients obtained using GA for Spring.

	Algorithm	$\mathbf{Z_p}$	$\mathbf{I_p}$	$\mathbf{P_p}$	$\mathbf{Z_q}$	$\mathbf{I_q}$	$\mathbf{P_q}$
Mar							
	GA	0.0068	0.0669	0.9263	2.7116	-1.4776	-0.2339
Apr							
	GA	0.0004	0.2052	0.7944	0.4799	2.0636	-1.5435
May							
	GA	0.0075	0.0440	0.9485	2.9376	-0.6875	-1.2501

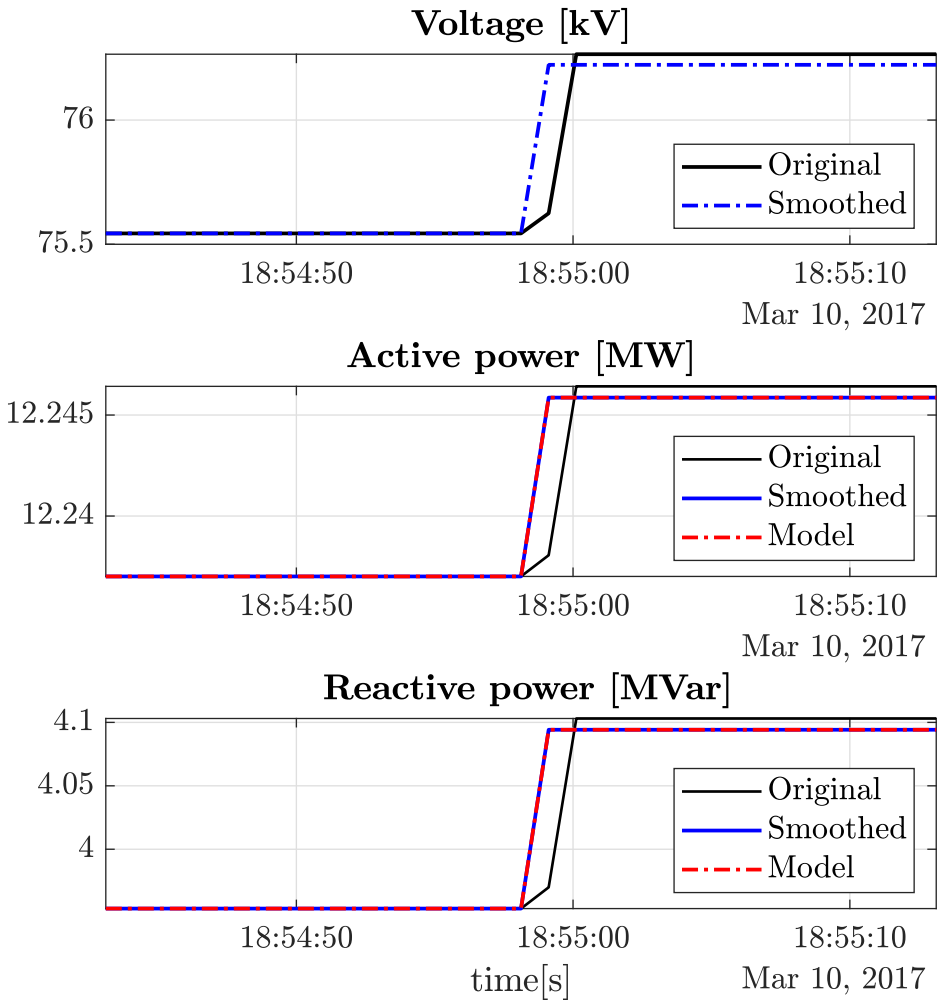

Figure A.2: Results of measurement based approach applying GA algorithm. The black signal corresponds to the actual or original signal obtained from the field measurements. The signal in blue represents the mean of the original signal before and after the event. The red signal corresponds to the fitted ZIP load model with the obtained parameters of March in table A.3.

Table A.4: Range of obtained load model coefficients for working days during the day time in Autumn.

$\mathbf{Z_p}$	$\mathbf{I_p}$	$\mathbf{P_p}$
(0.0004 - 0.0075)	(0.0440 - 0.2053)	(0.7944-0.9485)
$\mathbf{Z_q}$	$\mathbf{I_q}$	$\mathbf{P_q}$
(0.4799-2.7116)	(-1.4776 - -2.0636)	(-1.5435- -0,2339)

A.3 Summer-based study for evaluation point 3

Table A.5: ZIP load model coefficients obtained using GA for Summer.

	Algorithm	$\mathbf{Z_p}$	$\mathbf{I_p}$	$\mathbf{P_p}$	$\mathbf{Z_q}$	$\mathbf{I_q}$	$\mathbf{P_q}$
Jun							
	GA	0.0574	0.0084	0.9341	2.5791	-0.8880	-0.6911
Jul							
	GA	0.8994	0.1006	0	2.7230	-0.7004	-1.0226
Aug							
	GA	0.1738	0.5785	0.2476	1.6344	1.3446	-1.9789

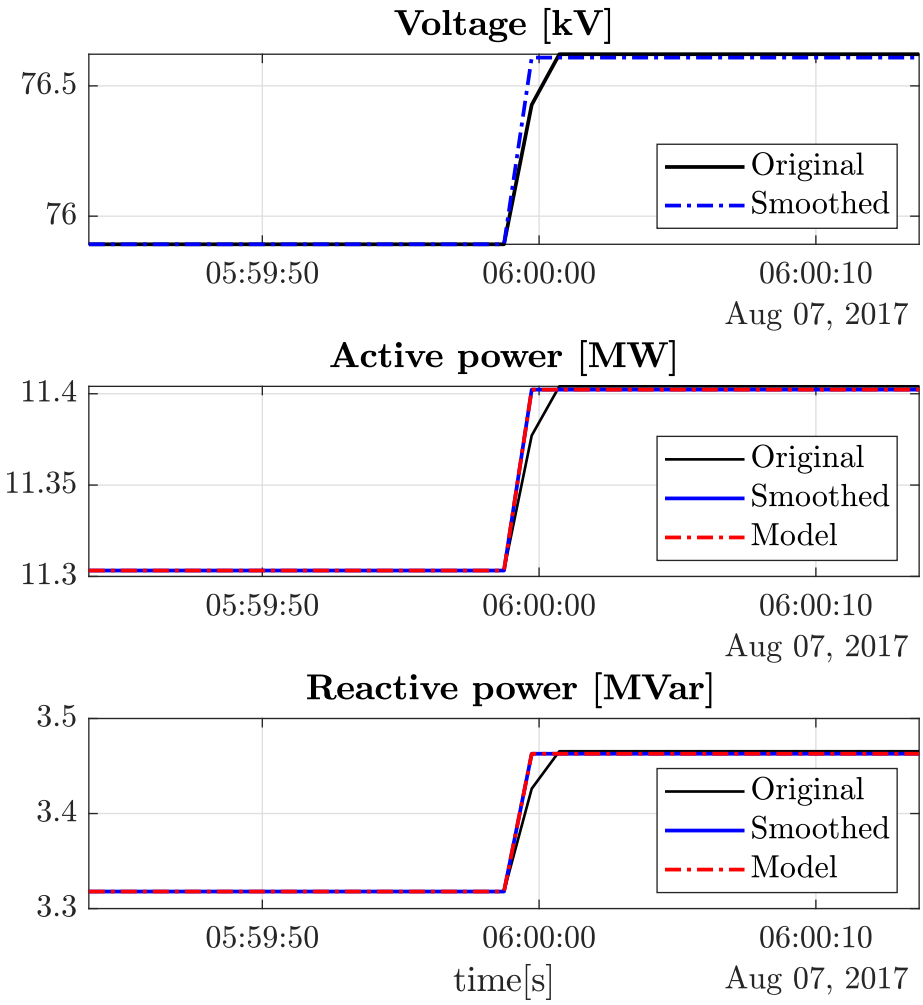

Figure A.3: Results of measurement based approach applying GA algorithm. The black signal corresponds to the actual or original signal obtained from the field measurements. The signal in blue represents the mean of the original signal before and after the event. The red signal corresponds to the fitted ZIP load model with the obtained parameters of August in table A.5.

Table A.6: Range of obtained load model coefficients for working days during the day time in Autumn.

$\mathbf{Z_p}$	$\mathbf{I_p}$	$\mathbf{P_p}$
(0.0574 - 0.8994)	(0.0084 - 0.5785)	(0 - 0.9341)
$\mathbf{Z_q}$	$\mathbf{I_q}$	$\mathbf{P_q}$
(1.6344 - 2.7230)	(-0.7004 - 1.3446)	(-0.6911 - -1.9789)

A.4 Autumn-based study for evaluation point 3

Table A.7: ZIP load model coefficients obtained using GA for Autumn.

	Algorithm	$\mathbf{Z_p}$	$\mathbf{I_p}$	$\mathbf{P_p}$	$\mathbf{Z_q}$	$\mathbf{I_q}$	$\mathbf{P_q}$
Sep							
	GA	0.0006	0.0246	0.9749	1.4775	0.5506	-1.0282
Oct							
	GA						
Nov							
	GA	0.2918	0.5966	0.1116	2.4637	0.0878	-1.5515

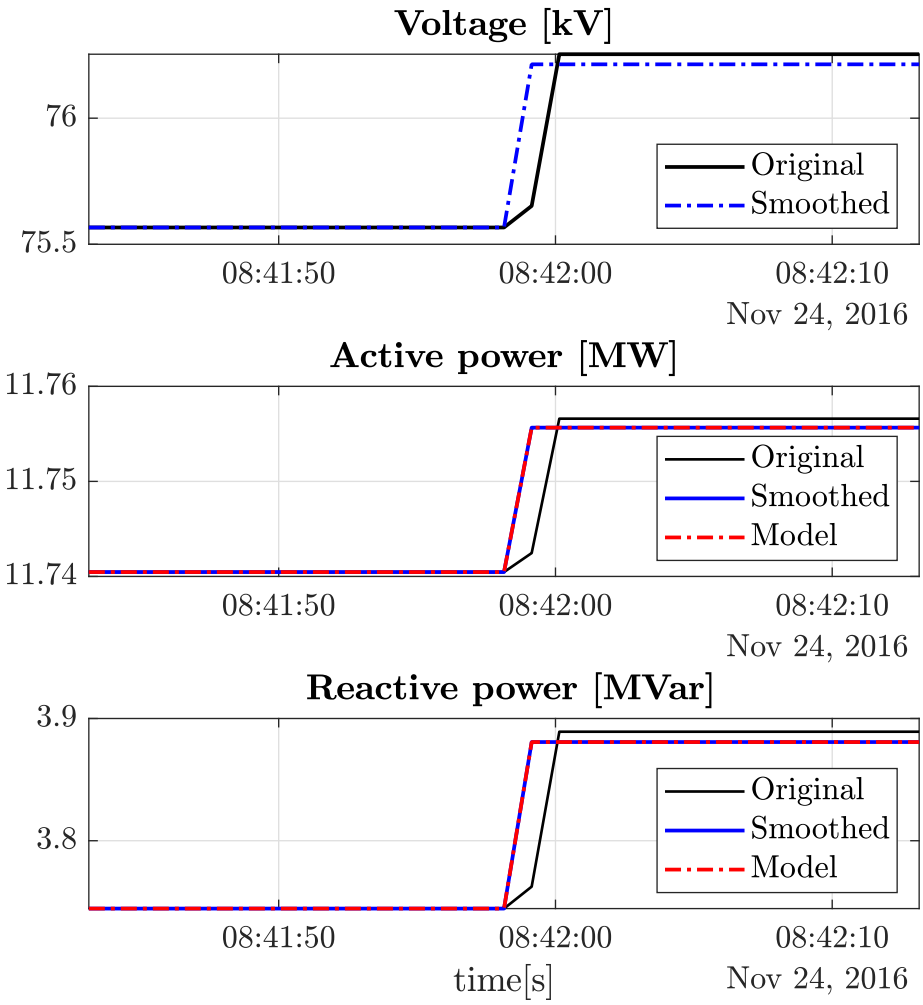

Figure A.4: Results of measurement based approach applying GA algorithm. The black signal corresponds to the actual or original signal obtained from the field measurements. The signal in blue represents the mean of the original signal before and after the event. The red signal corresponds to the fitted ZIP load model with the obtained parameters of November in table A.7.

Table A.8: Range of obtained load model coefficients for working days during the day time in Autumn.

$\mathbf{Z_p}$	$\mathbf{I_p}$	$\mathbf{P_p}$
(0.0006 - 0.2918)	(0.0246 - 0.5966)	(0.1116 - 0.9749)
$\mathbf{Z_q}$	$\mathbf{I_q}$	$\mathbf{P_q}$
(1.4775 - 2.4637)	(0.0878 - 0.5506)	(-1.5515 - -1.0282)

B

Appendix 2

B.1 Winter-based study for evaluation point 4

Table B.1: ZIP load model coefficients obtained using GA for Winter.

	Algorithm	$\mathbf{Z_p}$	$\mathbf{I_p}$	$\mathbf{P_p}$	$\mathbf{Z_q}$	$\mathbf{I_q}$	$\mathbf{P_q}$
Dec							
	GA	0.4656	0.3630	0.1715	0.7149	-1.4749	1.7600
Jan							
	GA	0	0.0001	0.9989	0.0318	-0.2863	1.2545
Feb							
	GA	0.0974	0.0332	0.8694	0.8188	-0.5229	0.7041

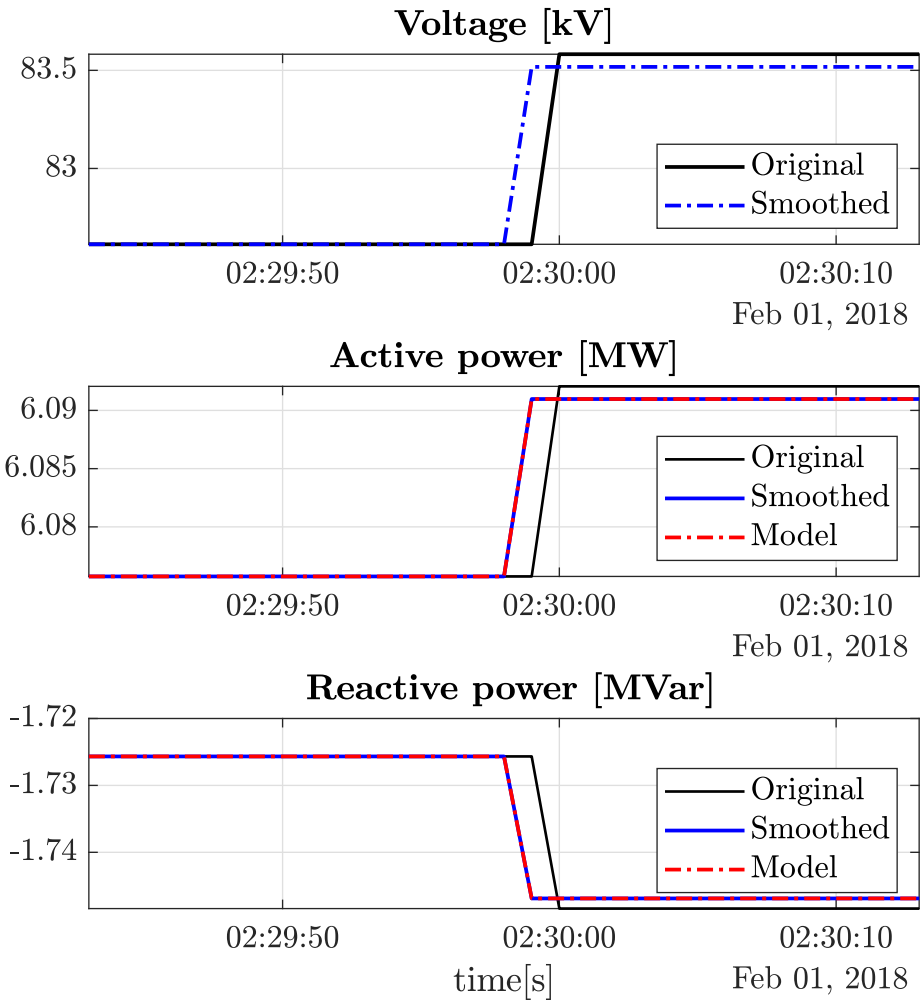

Figure B.1: Results of measurement based approach applying GA algorithm. The black signal corresponds to the actual or original signal obtained from the field measurements. The signal in blue represents the mean of the original signal before and after the event. The red signal corresponds to the fitted ZIP load model with the obtained parameters of February in table B.1.

Table B.2: Range of obtained load model coefficients for evaluation point 4 in Winter.

$\mathbf{Z_p}$	$\mathbf{I_p}$	$\mathbf{P_p}$
(0 - 0.4656)	(0.0001 - 0.3630)	(0.1715 - 0.9989)
$\mathbf{Z_q}$	$\mathbf{I_q}$	$\mathbf{P_q}$
(0.0318 - 0.8188)	(-1.4749- -0.2863)	(0.7041 - 1.7600)

B.2 Spring-based study for evaluation point 4

Table B.3: ZIP load model coefficients obtained using GA for Spring.

	Algorithm	$\mathbf{Z_p}$	$\mathbf{I_p}$	$\mathbf{P_p}$	$\mathbf{Z_q}$	$\mathbf{I_q}$	$\mathbf{P_q}$
Mar							
	GA	0	0	0	0	0	0
Apr							
	GA	0.2621	0.3251	0.4128	1.6218	-0.3587	-0.2631
Maj							
	GA	0.2306	0.4425	0.3270	0.2231	0.5000	0.2769

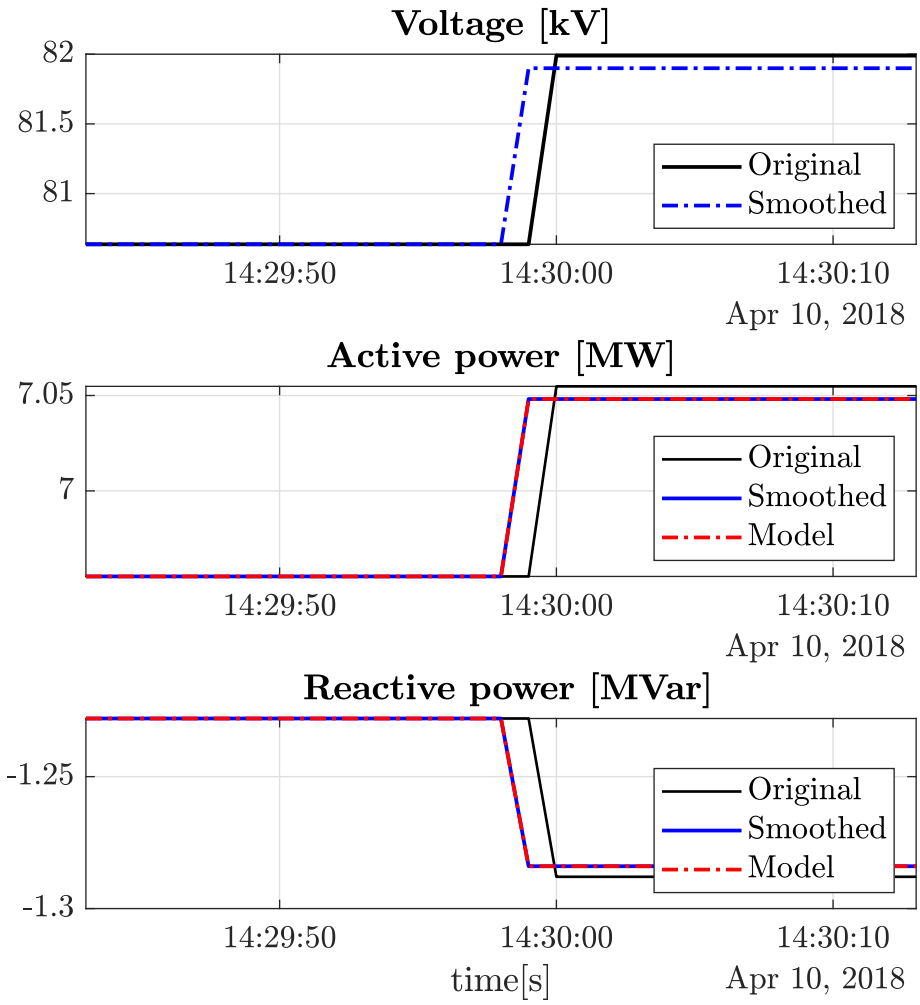

Figure B.2: Results of measurement based approach applying GA algorithm. The black signal corresponds to the actual or original signal obtained from the field measurements. The signal in blue represents the mean of the original signal before and after the event. The red signal corresponds to the fitted ZIP load model with the obtained parameters of April in table B.3.

Table B.4: Range of obtained load model coefficients for evaluation point 4 in Spring.

$\mathbf{Z_p}$	$\mathbf{I_p}$	$\mathbf{P_p}$
(0 - 0.2621)	(0 - 0.4425)	(0 - 0.4128)
$\mathbf{Z_q}$	$\mathbf{I_q}$	$\mathbf{P_q}$
(0 - 1.6218)	(-0.3587 - 0.5000)	(-0.2631 - 0.2769)

B.3 Summer-based study for evaluation point 4

Table B.5: ZIP load model coefficients obtained using GA for Summer.

	Algorithm	$\mathbf{Z_p}$	$\mathbf{I_p}$	$\mathbf{P_p}$	$\mathbf{Z_q}$	$\mathbf{I_q}$	$\mathbf{P_q}$
Jun							
	GA	0.1952	0.5007	0.3041	2.1795	0.3147	-1.4942
Jul							
	GA	0	0.0009	0.9981	0.0347	-0.0151	0.9805
Aug							
	GA	0.9988	0.0021	0.0001	-3.2181	-0.6656	4.8837

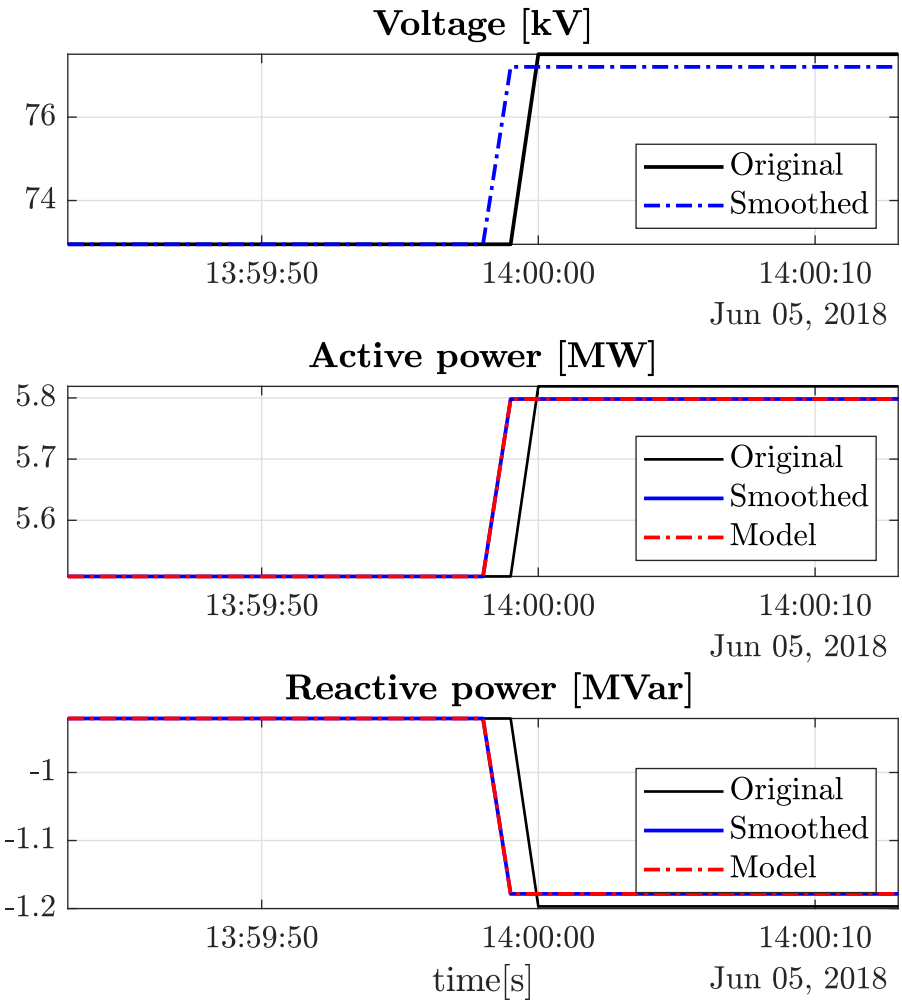

Figure B.3: Results of measurement based approach applying GA algorithm. The black signal corresponds to the actual or original signal obtained from the field measurements. The signal in blue represents the mean of the original signal before and after the event. The red signal corresponds to the fitted ZIP load model with the obtained parameters of June in table B.5.

Table B.6: Range of obtained load model coefficients for evaluation point 4 in Summer.

$\mathbf{Z_p}$	$\mathbf{I_p}$	$\mathbf{P_p}$
(0 - 0.9988)	(0.0009 - 0.5007)	(0.0001 - 0.9981)
$\mathbf{Z_q}$	$\mathbf{I_q}$	$\mathbf{P_q}$
(-3.2181 - 2.1795)	(-0.6656 - 0.3147)	(-1.4942 - 4.8837)

B.4 Autumn-based study for evaluation point 4

Table B.7: ZIP load model coefficients obtained using GA for Summer.

	Algorithm	$\mathbf{Z_p}$	$\mathbf{I_p}$	$\mathbf{P_p}$	$\mathbf{Z_q}$	$\mathbf{I_q}$	$\mathbf{P_q}$
Sep							
	GA	0.1657	0.5210	0.3133	0.8119	0.1563	0.0318
Oct							
	GA	0.9976	0.0033	0.0001	0	0	1
Nov							
	GA	0.9999	0.0011	0	-0.4388	0.8802	0.5586

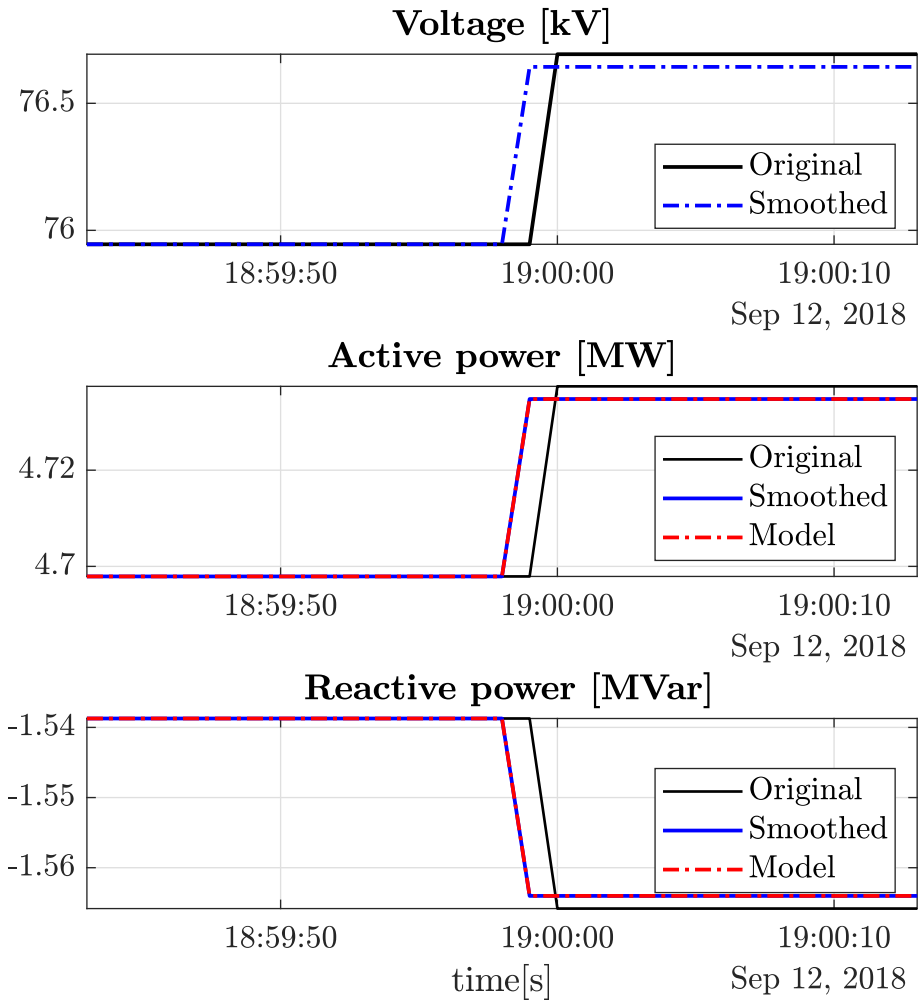

Figure B.4: Results of measurement based approach applying GA algorithm. The black signal corresponds to the actual or original signal obtained from the field measurements. The signal in blue represents the mean of the original signal before and after the event. The red signal corresponds to the fitted ZIP load model with the obtained parameters of September in table B.7.

Table B.8: Range of obtained load model coefficients for evaluation point 4 in Autumn.

$\mathbf{Z_p}$	$\mathbf{I_p}$	$\mathbf{P_p}$
(0.1657 - 0.9999)	(0.0011 - 0.5210)	(0 - 0.3133)
$\mathbf{Z_q}$	$\mathbf{I_q}$	$\mathbf{P_q}$
(-0.4388 - 0.8119)	(0 - 0.8802)	(0.0318 - 1)